Angewandte Chemie
Eine Zeitschrift der Gesellschaft Deutscher Chemiker

Supporting Information

Subcellular Duplex DNA and G-Quadruplex Interaction Profiling of a Hexagonal Pt^{II} Metallacycle

Olaya Domarco[+], Claudia Kieler[+], Christine Pirker, Carina Dinhof, Bernhard Englinger, Johannes M. Reisecker, Gerald Timelthaler, Marcos D. García, Carlos Peinador, Bernhard K. Keppler, Walter Berger,* and Alessio Terenzi**

anie_201900934_sm_miscellaneous_information.pdf
anie_201900934_sm_Video_S1.avi
anie_201900934_sm_Video_S2.avi

Table of Contents

Experimental Procedures

General

If not specified otherwise, chemicals were used in commercial grade (Sigma Aldrich and Thermo Fisher Scientific) from freshly opened containers. 5,10,15,20-Tetrakis(1-methyl-4-pyridinio)porphyrin tetra(p-toluenesulfonate) (TMPyP4) and solvents were purchased from Sigma Aldrich and used as received, without further purification. Pt-metallacycle **2** was synthesised as previously reported by us.[1] Mili-Q water was purified with a Milipore Gradient A10 apparatus. Merck 60 (230-400 mesh) silica gel was used for flash chromatography and Merck 60 F254 foils were used for thin layer chromatography. Proton and Carbon NMR spectra were recorded on a Bruker Avance 300 or a Bruker Avance 500 spectrometers. Mass spectrometry experiments were carried out in LCD-q-TOF Applied Biosystems QSTAR Elite spectrometer for low- and high-resolution ESI. Microwave-assisted reactions were carried out in an Anton Paar Monowave 300 reactor in a sealed reaction vial. The reaction mixture temperature was monitored via built-in IR sensor.
Buffers were prepared using MilliQ water and final pH values were measured using a Mettler Toledo pH-meter. Analysis and plotting of the data were carried out using Origin 9.5 (OriginLab Corp.), GraphPad Prism (version 5; GraphPad Software, San Diego, CA) and ImageJ 1.52g.[2]

The self-assembly of the final compound, having a hexagonal open box shape, occurred by mixing ligand **L1** with the platinum precursor $Pt(en)(NO_3)_2$ in water and using a microwave-assisted reaction at 150 °C for 3h.

Synthesis of 4,4'-([1,1'-biphenyl]-4,4'-diyl)bis(1-(2,4-dinitrophenyl)pyridin-1-ium)

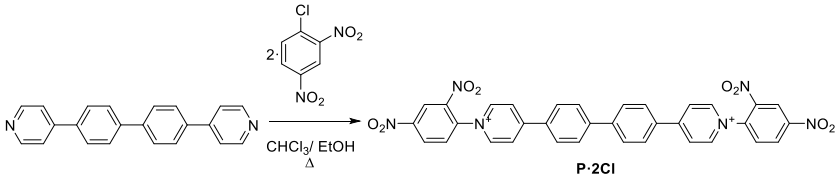

A solution of 4,4'-di(pyridin-4-yl)-1,1'-biphenyl (0.050 mg, 0.162 mmol) and 1-cloro-2,4-dinitrobenceno (0.098 mg, 0.486 mmol) in a mixture of EtOH/$CHCl_3$ 4:1 (25 mL) was heated at 90 °C for 72 hours. The solvent was removed under reduced pressure and the solid was washed with CH_2Cl_2 (10 mL) and CH_3CN (10 ml) to yield P·2Cl (48 mg, 48%). ^{1}H NMR (300 MHz, CD_3OD) δ (ppm): 9.32 (d, *J*= 2.5 Hz, 2H), 9.29 (d, *J*= 7.2 Hz, 4H), 8.96 (dd, *J*= 8.7, 2.5 Hz, 2H), 8.81 (d, *J*= 7.2 Hz, 4H), 8.39 (d, *J*= 7.1 Hz, 4H), 8.36 (d, *J*= 7.2 Hz, 4H), 8.18 (d, *J*= 8.5 Hz, 2H). HR-ESI-MS (m/z) calculated for $[M\text{-}2Cl]^+$ 2321.0744, found 321.0757.

Synthesis of L1·2NO$_3$

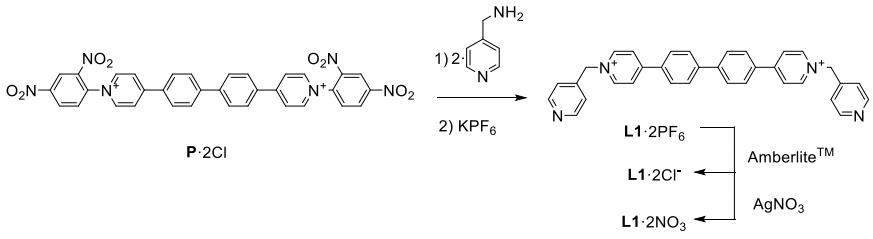

A solution of **P**·2Cl (80 mg, 0.07 mmol) and 4-(aminomethyl)pyridine (25 µL, 0.266 mmol) in MeOH (20 mL) was stirred overnight at room temperature. The solvent was removed under reduced pressure to obtain a solid residue, which was subjected to flash chromatography (SiO_2, CH3CN/NaCl (aq.)(0.6 M)/MeOH 4:1:1). The ligand containing fractions were combined, evaporated, dissolved in water and the obtained yellow solid was filtered. This solid was re-dissolved in the minimum amount of MeOH and an excess of KPF_6 was added to yield **L1**·2PF_6 (40 mg, 47%) ^{1}H NMR (500 MHz, CD_3CN) δ (ppm): 8.78 (d, *J*= 7.1 Hz, 4H), 8.71 (d, *J*= 6.1 Hz, 4H), 8.40 (d, *J*= 7.1 Hz, 4H), 8.13 (d, *J*= 8.7 Hz, 4H), 8.06 (d, *J*= 8.7 Hz, 4H), 7.35 (d, *J*= 6.0 Hz, 4H), 5.78 (s, 4H). ^{13}C NMR (125 MHz, CD_3CN) δ (ppm): 156.41 (C), 150.72 (CH), 144.87 (CH), 142.99 (C), 141.96 (C), 133.50 (C), 129.02 (CH), 128.48 (CH), 125.47 (CH), 122.80 (CH), 62.13 (CH_2). HR-ESI-MS (m/z) calculated for $[M\text{-}2PF_6]^{+2}$ 246.1151, found 246.1176.
L1·2PF_6 and Amberlite CG-400 (200 mg) were suspended into H_2O/MeOH (1:1, 50 mL), and stirred for 12 h. The resin was removed by filtration and the solvent was removed under reduced pressure to yield **L1**·2Cl (22 mg, 34%). A solution of **L1**·2Cl (22 mg, 0.039 mmol) and $AgNO_3$ (13.3 mg, 0.078 mmol) in H_2O/MeOH (1:1, 30 mL) was stirred at 25 ° for 12 h in the dark. The mixture was filtered and the filtrate was slowly evaporated to yield **L1**·2NO_3 (21.5 mg, 90%). ^{1}H NMR (500 MHz, D_2O) δ (ppm): 8.93 (d, *J*= 7.0 Hz, 4H), 8.62 (d, *J*= 6.3 Hz, 4H), 8.45 (d, *J*= 7.0 Hz, 4H), 8.13 (d, *J*= 8.6 Hz, 4H), 8.04 (d, *J*= 8.6 Hz, 4H), 7.42 (d, *J*= 6.3 Hz, 4H), 5.92 (s, 4H).

^{13}C NMR (125 MHz, D_2O) δ (ppm): 156.67 (C), 149.64 (CH), 144.65 (CH), 143.15 (C), 142.84 (C), 133.36 (C), 128.82 (CH), 128.25 (CH), 125.22 (CH), 123.10 (CH), 62.01 (CH_2).

Synthesis of 1·8NO$_3$

A suspension of **L1**·2NO_3 (40 mg, 0.068 mmol) and (en)Pt(NO_3)$_2$ (24.2 mg, 0.068 mmol) in H_2O (20 mL), was heated at 150 °C for 3 h using microwave-assisted heating. The resulted suspension was transferred into a round-bottom flask and the solvent was removed under reduced pressure to obtain a yellow solid (yield 95 %). ^{1}H NMR (500 MHz, D_2O) δ (ppm): 8.86 (d, *J* = 6.9 Hz, 8H), 8.83 (d, *J* = 6.8 Hz, 8H), 8.24 (d, *J* = 7.0 Hz, 8H), 7.87 (d, *J* = 8.6 Hz, 8H), 7.74 (d, *J* = 8.5 Hz, 8H), 7.67 (d, *J* = 6.9 Hz, 8H), 5.92 (s, 8H) 2.88 (s, 8H). ^{13}C NMR (125 MHz, D_2O) δ (ppm): 157.58 (C), 152.68 (CH), 146.83 (C), 145.49 (CH), 144.95 (C), 134.00 (C), 129.15 (CH), 128.63 (CH), 127.20 (CH), 126.04 (CH), 47.34 (CH_2).

1·8NO$_3$ (10 mg) was re-dissolved in the minimum amount of H_2O (2 mL) and an excess of KPF_6 was added to yield **1·8PF$_6$** as a yellow precipitate which was then filtered, washed with cold water (30 mL) and dried under vacuum. HR-ESI-MS (m/z) calculated for [M-3PF_6-H]$^+$ 21109.1709, found 1109.1837; calculated for [M-4PF_6-2H]$^+$ 21036.1849, found 1036.1942; calculated for [M-3PF_6]$^+$ 3739.783, found 739.7902; calculated for [M-4PF_6-H]$^+$ 3691.1257, found 691.1281; calculated for [M-5PF_6-2H]$^{+3}$ 642.4683; found 642.4689.

Interaction with G4 and B-DNA in solution

Steady State Absorption and Emission Spectroscopy. UV-Vis spectra overtime on a PerkinElmer LAMBDA 35 and Jasco V-650 spectrophotometers using 1 cm path-length quartz cuvettes. Fluorescence spectra were recorded on Horiba FluoroMax-4 and Fluoromax Plus-P spectrofluorometers (Kyoto, Japan). Scans were run at room temperature with excitation and emission slit widths as reported in the captions of the corresponding pictures.

For quantum yield measurements, all samples were freshly prepared. Absorption and emission spectra were recorded for samples with concentrations in the range 0.2−5 μM, where the absorption was between 0.01 and 0.08. Quantum yields were determined using quinine sulfate in 0.1 M H_2SO_4 as reference (with φ_F = 0.55 at λ_{exc} = 365 nm and λ_{em} = 451 nm).

Lifetime Measurements. Time-correlated single photon counting (TCSPC) measurements were carried out on a Fluoromax-4 apparatus equipped with a SPC Controller (FluoroHub, Horiba Jobin Yvon). The selected excitation source was a Horiba Nanoled N-370 (pulse < 1.2 ns). A 0.01% dilution of Ludox AS40 colloidal silica in purified water was used as prompt. Data were finally fitted using least squares methods with DAS6 Fluorescence Decay Analysis Software.

DNA sequences for binding studies. The oligodeoxynucleotides (ODNs) reported in Table S2 were purchased from IDT (Integrated DNA Technologies) in HPLC purity grade.

They were resuspended in IDTE buffer (10 mM Tris, 0.1 mM EDTA, pH 8.0, where Tris (tris-hydroxymethyl-aminomethane) is the actual buffer while EDTA (ethylenediaminetetraacetic acid) prevents DNA digestion by nuclease) to obtain 100 μM stock solutions. The extinction coefficient values at 260 nm provided by the manufacturer were used to determine the final ODNs strand concentration.

Lyophilized calf thymus DNA (ct-DNA) was purchased from Sigma-Aldrich and resuspended in IDTE buffer. Final DNA concentration in bases was determined by UV spectrophotometry using 6600 M^{-1} cm^{-1} as molar absorption coefficient at 260 nm.

All along the text, concentration of DNA sequences is reported as strand molarity. When explicitly stated, ODN concentrations were reported in bases.

FRET melting assay. FRET experiments were performed on a 96-well format Applied Biosystems® 7500 Real-Time PCR cycler equipped with a FAM (6-carboxyfluorescein) filter (λ_{ex} = 492 nm; λ_{em} = 516 nm). ODNs were purchased with the probes FAM and TAMRA (6-carboxy-tetramethylrhodamine) attached at the 5'- and 3'- ends, respectively.

To afford G4 folding, FRET ODNs stock solutions were diluted to the desired concentration using 60 mM potassium cacodylate buffer (pH 7.4) and then heated to 95 °C for 5 min, followed by slowly cooling to room temperature overnight. In the final mixes, ODNs final concentration was set to 0.2 μM (total volume of 30 μl). Control TMPyP4 was previously dissolved in DMSO to give 1 mM stock solutions and further diluted with the buffer reaching a total percentage of DMSO never above 0.1 %.

The melting of *c-Kit2* and *h-Telo* G4s (0.2 μM) stabilised by Pt metallacycle **1** was also monitored in a competition assay in the presence of increasing concentration of a non-fluorescent DNA structure. In particular ct-DNA was used to represent a duplex structure while the sequence G4-nl was selected for a quadruplex with no loops.

FAM emission data were collected in duplicate or triplicate in the range 25-95 °C (with a ramp of 1 °C every 30 s). To compare different sets of data, emission data were normalised.[3] $T_{1/2}$ is defined as the temperature at which the normalised emission is 0.5.

Circular dichroism. CD spectra were recorded on Chirascan™ CD (by AppliedPhotophisics), using 1 cm path-length quartz cuvettes, at room temperature using the following parameters: bandwidth: 1.0 nm, time per point: 0.5 s, repeats: 4. The titrations were carried out by adding increasing amounts of **1** to the selected ODN at constant concentration.

Molecular Modelling. Molecular docking was carried out using AutoDock Vina 1.1.2.[4] PDB IDs 2KQH and 1BNA were used as models for *c-Kit2* and B-DNA quadruplexes, respectively.

The structure of compound **1** was optimised by DFT using B3LYP functional,[5–7] Lanl2dz pseudopotential basis set for platinum,[8] and 6-31G(d,p) basis set for the other atoms.[9,10] Calculations were performed with Gaussian09.[11]
Autodock Tools package was used to prepare receptors and the platinum SCC for docking calculations.[12] A grid box large enough to contain the whole DNA structure was created. Since Vina formally treats metals as H-bond donors and no significant changes were expected, Pt(II) was changed with Ni(II) just to retain the square planar coordination around the metal centre. Figures were rendered using Chimera software.[13]

Cell studies

Cell Culture. The human cancer cell lines U2OS, MCF-7, T98G, and U373MG (compare Table S2) were purchased from American Type Culture Collection (Manassas, VA, USA) and cultured in respective growth media (U2OS in IMDM, MCF-7 in DMEM, T98G and U373MG in MNP medium), supplemented with 10% fetal bovine serum (FBS South America, Biowest, Nuaillé, France). VM-1 cells were obtained from the Institute of Cancer Research (Vienna, Austria) and grown in RPMI-1640, supplemented with 10% FBS. Non-malignant human lung fibroblasts (HLF) were taken in culture from a surgical pneumothorax specimen at the ICR Vienna and non-transformed HaCaT keratinocytes were donated by Prof. Fusenig, DKFZ Heidelberg, Germany. All cells cultures were incubated at 37 °C and 5% CO_2 and regularly screened for *Mycoplasma* contamination (Mycoplasma Stain kit, Sigma, St. Louis, Missouri, USA).

Cell viability assays (MTT). 2-3x10^4 cells/ml were seeded in 96-well plates and left to adhere overnight. Cells were treated with 0-50 µM of metallacycle **1** and its ligand **L1** for 72h, followed by determination of cell viability by the 3-(4,5-dimethylthiazol-2-yl)-2,5-diphenyltetrazolium bromide (MTT)-based vitality assay (EZ4U, Biomedica, Vienna, Austria) according to the manufacturer's instructions. Concentrations of **1** and **L1** leading to a reduction of cell number by 50% (IC_{50}) were calculated from whole dose-response curves generated by GraphPad Prism 5 software. Each data point in the response curves represents the mean ± SD of three replicates of one representative experiment, which was performed at least three times. Interaction of **1** with both ThT and PDS was done in 72 h co-exposure assays and cell viability again determined by MTT assay. To investigate a possible interaction between **1**- and cisplatin (Cis) on (Cis)-mediated anticancer activities, co-exposure experiments were performed at the indicated concentrations of both compounds. MTT assay - detecting mitochondrial activity - might be prone for misleading results (overestimation of cell viability) in case of cisplatin. This DNA-damaging compound frequently induces in malignant cells a cell cycle arrest in G2 phase with massive enlarging of cell bodies but lack of apoptosis induction. Hence, we used in these experiments instead of MTT assays the CellTiter-Glo® Luminescent Cell Viability Assay (Promega) detecting cellular ATP contents following the instructions of the manufacturer. The other settings were kept as in MTT assays.

Clonogenic assay. 1-2x10^3 cells/ml were seeded in 24-well plates and incubated overnight, followed by treatment with 0-20 µM of **1** and **L1**. After 7-day drug exposure, cells were fixed with MeOH and stained with crystal violet (0.1 mg/ml in PBS). Images of each well were taken (Nikon Digital Camera D3200, Minato, Tokyo, Japan) and plates were scanned on a Typhoon scanner (Typhoon TRIO Variable Mode Imager, GE Healthcare Life Sciences). Colony growth was determined by calculating integrated area densities with the ImageJ 1.51f software (Wayne Rasband, National Institutes of Health, USA).

Drug uptake and cell cycle analysis by flow cytometry. U2OS cells resuspended in PBS were treated with 50 µM **1** and **L1** for 1h**.** Fluorescence intensity measurements were carried out on a LSRFortessa flow cytometer (BD Biosciences, East Rutherford, NJ, USA), using 405 nm laser excitation and 450/50 nm (“Horizon V450”), 605/12 nm (“Qdot 605”), and 655/8 nm (“Qdot 655”) bandpass emission filters, as well as 355 nm laser excitation and a 450/50 nm (“DAPI”) bandpass emission filter. For longer-term drug uptake measurements, U2OS cells were resuspended in serum-free RPMI 1640 media (Sigma-Aldrich, Missouri, USA), containing 3-(N-morpholino)propanesulfonic acid (MOPS; Sigma-Aldrich) and 4-(2-hydroxyethyl)-1-piperazineethanesulfonic acid (HEPES; Sigma-Aldrich, Missouri, USA). Cells were treated with indicated concentrations of **1** and **L1** or with **1** in combination with the indicated concentrations of cisplatin (Cis, 2mM stock prepared in PFS, Sigma) or pyridostatin (PDS, 10 mM stock in DMSO, Sigma) and fluorescence intensity was measured by flow cytometry using 405 nm laser excitation and the Horizon V450 bandpass emission filter at the indicated time points. Data were analysed using Flowing Software 2.5.1 (Perttu Terho, Turku, Finland). For cell cycle analysis, 2x10^5 cells/well were seeded into 6-well plates. After overnight incubation, cells were treated with indicated concentrations of **1** and **L1**. After 24h drug exposure, cells were fixed with 70% ice-cold EtOH at -20°C overnight. Fixed cells were treated with RNase A (0.79 Kunitz units/ml, Sigma-Aldrich, Missouri, USA) for 30 min at 37°C and stained with propidium iodide (1 mg/ml in PBS; Sigma-Aldrich, Missouri, USA) for 30 min at 4°C. Fluorescence intensity was measured by flow cytometry and quantified with the Cell Quest Pro Software (BD Biosciences).

Metaphase chromosome preparation. Metaphase chromosome preparation of MCF-7 cells was performed according to standard protocols and as described by Pirker et al.[14]

Emission fingerprinting with lambda stacks. MCF-7 cells fixed with MeOH were incubated with either 50 µM 1 or L1 for 30 min at RT. After washing with 1x PBS, cells were mounted with Vectashield (Vector Laboratories, Inc., Burlingame, CA, USA) without DAPI. Lambda stacks for **1** and **L1** were acquired with a Zeiss LSM 780 confocal microscope and Zen 2.3 SP1 software (Carl Zeiss microscopy, Germany) using a Plan-Apochromat 63×/1.4 NA Oil DIC M2763x objective with immersion oil and 405 nm laser line. The emission of the drugs was determined in the range of 411-687 nm with a bandwidth of 9 nm. Data were evaluated with Zeiss Zen 2.1

software (Carl Zeiss). Emission spectral profiles were obtained using the linear unmixing tool by normalizing the signal intensity values and plotting them on a linear graph versus the corresponding emission wavelengths.

Live Cell Microscopy. 3-5x10^4/ml cells were seeded in 8-well chamber slides (Ibidi, Martinsried, Germany). After overnight incubation, cells were either additionally pre-treated for 24h with 1 µM TMPyP4 or cells were treated directly with the indicated concentrations of **1** and **L1**. Alternatively, cells were pretreated for 30 min with the G-quadruplex probe 5 µM Thioflavin T (ThT, Sigma) followed by addition of 5 µM **1**. Images were taken every 30 minutes over a period of 24h (29h for Video S1) on a live cell microscope (Visitron Systems, Puchheim, Germany) using a Plan-Apochromat 40×/1.4 NA Oil DIC M27 objective and the imaging software VisiView®. Lumencor (Beaverton, USA) spectra colour LEDs were used for fluorescence illumination (395/25 nm excitation and 460/50 nm bandpass emission filter for blue, 475/34 nm excitation and 525/50 nm emission filter for green and 640/30 nm excitation and 700/75 nm emission filter for red. Images were captured with a PCO Edge 4.2 sCMOS camera and quantified using ImageJ 1.51f software (Wayne Rasband, National Institutes of Health, USA).

Fluorescence microscopy. Cells were seeded in 8-well chamber slides with removable silicone walls (Ibidi). After overnight incubation, cells were stained and/or fixed in different sequences as appropriate and indicated in the respective figure legends. Alternatively, for nuclear staining cells were in some cases cytospin prepared instead of being grown on chamber slides. For staining and competition experiments with specific G-quadruplex probe Thioflavin T (ThT, Sigma), nucleolar probe SYTO® RNASelect green (SYTO, Molecular Probes, Eugene, OR) and MitoTracker® Red CMXRos mitochondrial stain (250nM; Molecular Probes) cells were fixed in MeOH (-20°C, 15 min). Fluorescence images were taken on a DMRXA (Leica, Wetzlar, Germany) equipped with a monochrome fluorescence camera based on a CCD sensor and a HCX PL APO 63x (1.32 – 0.6) or a PL APO 100x (1.4 – 0.7) oil objective using DAPI (λ_{exc} 350/50, λ_{em} 460/50), FITC (λ_{exc} 495/25, λ_{em} 537/29), or Cy3 (λ_{exc} 546/22, λ_{em} 590/23) filter cubes. Photomicrographs were processed by VisiView software (Visitron Systems, Puchheim, Germany) at the indicated settings. For photobleaching experiments, **1**-stained cells were exposed for longer periods to UV excitation. Fluorescence images were taken with a PL APO 100x (1.4 – 0.7) oil objective in time-lapse mode with one frame every 5 seconds at an illumination time of 10 ms and the DAPI filter cube (350/50 excitation, 460/50 emission). Photomicrographs were processed by VisiView software (Visitron Systems, Puchheim, Germany) at Max/Min (range) autoscale settings.

Confocal laser-scanning microscopy (CLSM). 3-7x10^4/ml U2OS and MCF-7 cells were seeded in 8-well chamber slides with removable silicone walls (Ibidi). After overnight attachment, staining with **1** was performed either in living or in fixed cells. For fixation with PFA, cells were washed with 1xPBS before adding a 4% PFA containing PBS solution for 30min at RT. Following PFA quenching with a PBS-solution containing 0.1 M glycin, cells were washed with 1xPBS and subsequent permeabilisation was carried out using 0.1% Triton-X-100 in 1xPBS for 15min at RT. After washing again with 1xPBS, cells were used for immunofluorescence staining. For fixation with MeOH, washed cells were air-dried at least 1 hour before adding ice-cold MeOH for 10 min at -20°C. Following PBS-washing, cells were ready for subsequent staining procedures. For live cell staining, cells were treated with 50 µM **1** for 30-60 min at 37°C before fixation. Staining of fixed cells as well as metaphase chromosome spreads was performed by adding a 50 µM drug dilution in 1xPBS for 30 min at RT. For immunofluorescence staining, MeOH-/ PFA-fixed cells as well as metaphase chromosome preparations were blocked for 45min at RT with 1x PBS-BSA (0.2%) containing 10% FBS (for PFA fixed cells, 0.1% Triton-X-100 was additionally added to the blocking buffer). Blocked cells were incubated with BG4 antibody[15,16] (Mouse IgG1, from AbsoluteAntibody) diluted 1:200 in 1x PBS-BSA (0.2%) and 3% FBS (for PFA fixed cells 0.1% Triton-X-100 was additionally added to the antibody dilution) and incubated overnight at 4°C. After washing with 1x PBS, cells were incubated with secondary AB (AF594, Thermo Fisher Scientific, Waltham, MA, USA) diluted 1:500 in 1x PBS-BSA (0.2%) and 3% FBS (for PFA fixed cells 0.1% Triton-X-100 was added) for 1h at 37°C or RT. When indicated, cells or metaphase chromosome spreads were further counterstained with 50 µM **1** or **L1** for 30 min at RT. For counterstaining with 4′,6-diamidino-2-phenylindole (DAPI, Thermo Fisher Scientific, Waltham, MA, USA), fixed nuclei and metaphase chromosomes were either incubated for 10 min with 1.5 µg/ml DAPI at RT or slides were mounted with Vectashield containing 1.5 µg/ml DAPI (Vector Laboratories, Inc., Burlingame, CA, USA). Samples were stored in the dark at 4°C until subsequent analysis with a Zeiss LSM700 confocal microscope (Carl Zeiss microscopy, Germany) for fluorescence imaging in DAPI (405 nm excitation and 450/90 nm emission) and AF594 (555 nm excitation and >585 nm emission) channels with a Plan-Apochromat 63×/1.4 NA Oil DIC M27. Transmitted light images were acquired with the 405 nm violet laser line in DICIII with T-PMT. For super-resolution imaging, a Zeiss LSM 880 microscope equipped with an Airyscan detector, a laser diode for 405 nm excitation, a BP 420-480 emission filter and a 63x/1.40 Plan-Apochromat, Oil, DIC III objective was used. Micrographs were evaluated with Zeiss Zen 2010 B SP1 software (Carl Zeiss).
Three-dimensional surface plots of single pixel intensities, derived from inverted DIC images of cropped nuclei were generated using the "3D Surface Plot" plugin in the FIJI distribution package of ImageJ software. Two-dimensional pixel intensity plots from lines indicating the region of interest in fluorescence and DIC channels were generated using the "Plot Profile" analysis tool in ImageJ software.

mRNA expression microarray. The impact of **1** (25 µM, 24 h exposure) and PDS (15 µM, 24 h exposure) on whole-genome gene expression was performed on 4×44K whole genome oligonucleotide-based gene expression arrays (Agilent, Santa Clara, USA) as previously described.[17,18] Gene expression data were preprocessed in R using the LIMMA package and evaluated by gene set enrichment analysis (GSEA) (http://www.broadinstitute.org/gsea/msigdb/index.jsp) against the KEGG database gene sets. Additionally, the set of genes located in chromosomal regions enriched for G4 structures was derived from supplementary Table S4 in Lam et al. 2012.[19]

Statistical analysis. Data were analysed using GraphPad Prism. If not specified otherwise, data are given as mean values ± standard deviation (SD) of triplicate values of one representative experiment, performed at least three times. For comparison of two groups, two-tailed Student's t-test was carried out. P-values, t-values (t) and degrees of freedom (DF) of each analysis are indicated in corresponding figure legends. Comparison of multiple groups was performed using one-way analysis of variance (ANOVA) with Bonferroni post-test. P-values below 0.05 were considered as statistically significant and marked with asterisks: *** $p < 0.001$.

Table S1. IC_{50} values for **1** and **L1**

Cell line	U2OS		MCF-7		VM-1		U373MG		T98G		HaCaT		HLF	
	Mean IC_{50}	± SD	Mean IC_{50}	± SD	Mean IC_{50}	± SD	Mean IC_{50}	± SD	Mean IC_{50}	± SD	Mean IC_{50}	± SD	Mean IC_{50}	± SD
L1*	35.58	4.64	35.47	1.55	>50	-	44.14	3.13	43.30	1.08	>50	-	36.43	8.31
1	31.67	3.21	29.81	4.64	45.34	2.07	35.85	3.56	37.28	1.41	>50	-	26.04	5.21

* While **L1** and **1** showed similar IC_{50} values in the MTT tests, when observed in live-cell imaging, metallacycle **1** revealed a higher tendency to induce cell death.

Table S2. 5'-3' ODNs sequences. In *ds-DNA* Heg linker is [(-CH_2-CH_2-O-)$_6$]

ODN	Sequence
h-Telo	AGG GTT AGG GTT AGG GTT AGG G
c-Kit1	AGG GAG GGC GCT GGG AGG AGG G
c-Kit2	CGG GCG GGC GCG AGG GAG GGG
hTERT	GGG GGC TGG GCC GGG GAC CCG GGA GGG GTC GGG ACG GGG CGG GG
hTERT-s	AGG GGA GGG GCT GGG AGG GC
Bcl2	AGG GGC GGG CGC GGG AGG AAG GGG GCG GGA GCG GGG CTG
VEGF	CGG GGC GGG CCT TGG GCG GGG T
ds-DNA (duplex)	TATAGCTATA-Heg-TATAGCTATA

Table S3. Overview of the different cell lines used in this project

Cell line	Disease	Tissue	Growth medium	Source
U2OS	Osteosarcoma	Bone	IMDM (Sigma-Aldrich)	ATCC
MCF-7	Adenocarcinoma	Mammary gland, breast	DMEM (Sigma-Aldrich)	ATCC
T98G	Glioblastoma	Brain	MNP (Sigma-Aldrich)	ATCC
U373MG	Glioblastoma	Brain	MNP (Sigma-Aldrich)	ATCC
VM-1	Melanoma	Skin	RPMI 1640 (Sigma-Aldrich)	ICR[20]
HaCaT	Keratinocytes, non-malignant	Skin	RPMI 1640 (Sigma-Aldrich)	Prof. Fusenig, DKFZ Heidelberg
HLF	Fibroblasts, non-malignant	Lung; pneumothorax	RPMI 1640 (Sigma-Aldrich)	ICR

VM: Vienna Melanoma
IMDM: Iscove's Modified Dulbecco's Medium
DMEM: Dulbecco's Modifies Eagle's Medium
MNP: Modified Eagle's Medium supplemented with 0.2% Na-pyruvate and 1% non-essential amino acids
RPMI: Roswell Park Memorial Institute
ATCC: American Type Culture Collection
ICR: Institute for Cancer Research, Vienna

Results and Discussion

Spectroscopic features of metallacycle 1

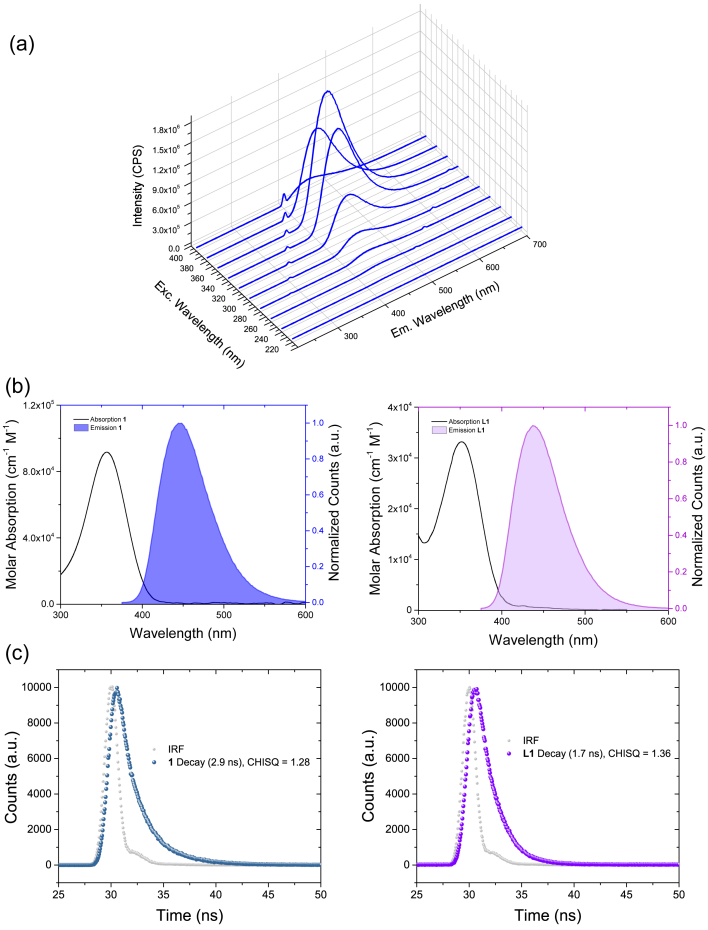

Figure S1. Fluorescence emission of metallacycle 1 and its ligand L1. (a) Full excitation-emission 3D landscape of 5 μM **1** in Tris-HCl 5 mM, KCl 50 mM, pH=7.8, obtained by fluorescence spectroscopy (Slit width: 0.5 nm). Spectra are shown for excitation wavelengths from 220 nm to 400 nm. 1st and 2nd order Rayleigh scattering can be seen as diagonal ridges. (b) Absorption (black) and emission (filled area) spectra of **1** and **L1** in Tris-HCl 5 mM, KCl 50 mM, pH=7.8. (c) Excited state lifetime decay for **1** and L**1** in Tris-HCl 5 mM, KCl 50 mM (pH=7.8) measured in a time-correlated single photon counting (TCSPC) setup. Both compounds exhibit a mono-exponential decay (violet and blue dots). IRF (grey dots) = instrument response function (prompt).

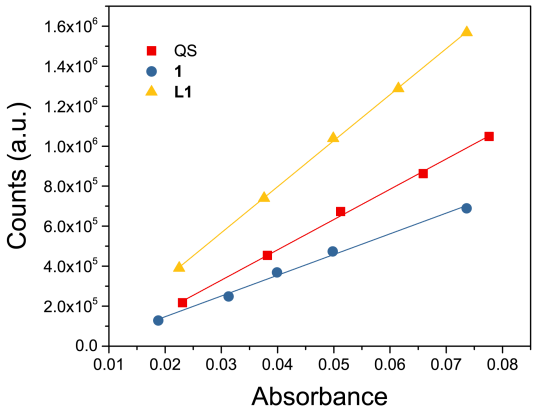

Figure S2. Quantum yield evaluation of 1 and L1. Plot of emission vs absorption in water of **1**, **L1** and quinine sulfate (QS) for quantum yield evaluation.

Stability of metallacycle 1

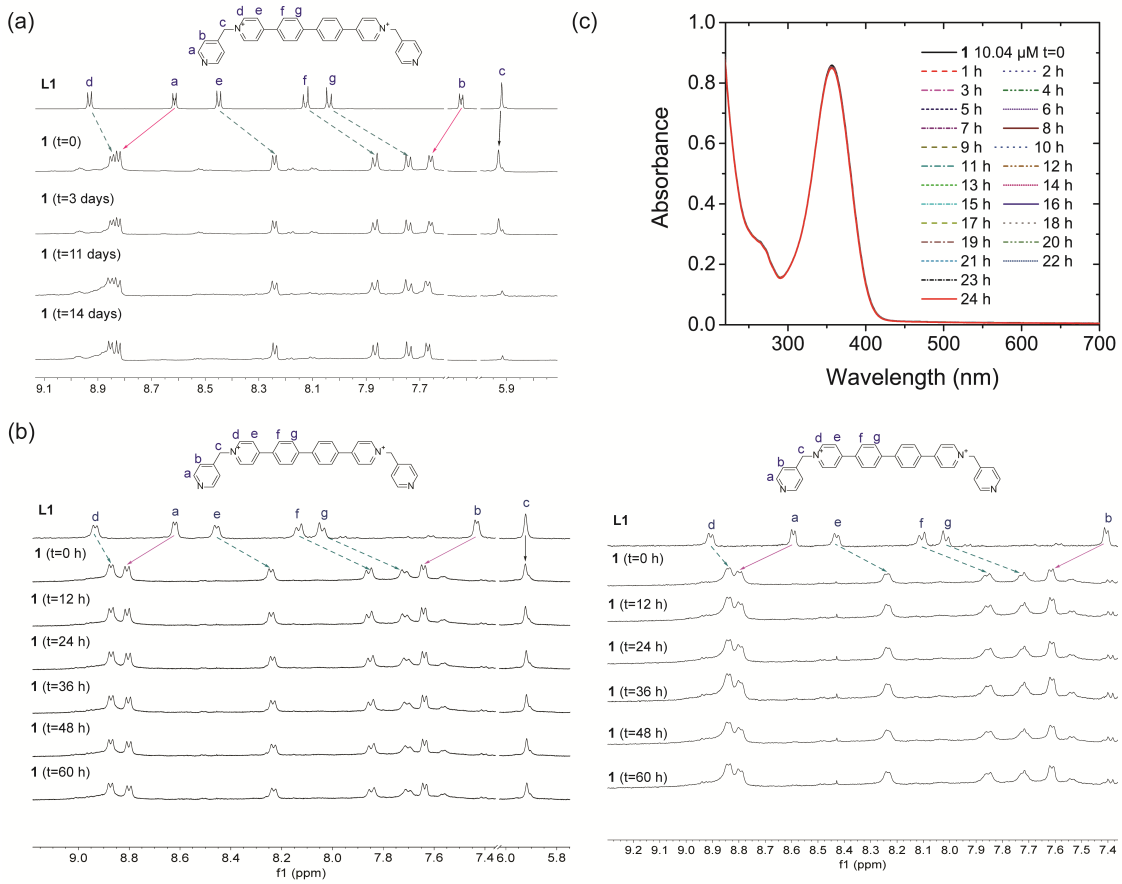

Figure S3. Stability overtime of compound 1. (a) NMR spectra of **1** overtime in (a) D_2O and (b) cell culture medium RPMI without (left) and with (right) fetal bovine serum (with 10% D_2O) (b) UV-Vis spectra of **1** overtime in the buffer Tris-HCl 5 mM, KCl 50 mM (pH=7.8).

Duplex DNA vs G4 binding studies

At first, we assessed the capacity of our platinum compound **1** and its constituent ligand **L1** to bind/stabilise duplex and/or quadruplex DNA. A standard FRET assay was performed using a self-complementary duplex model and the typical telomeric sequence *h-Telo*, arranged in a hybrid G4 topology.[21] Ligand **L1** did not affect the melting temperature of the duplex and had a minor influence on the stability of the quadruplex when compared to **1** (Figure S4). The metallacycle strongly stabilised the telomeric G4 ($\Delta T_{1/2}$ = 24.9) and, four time less the duplex ($\Delta T_{1/2}$ = 7.2) at the same concentration. The stabilisation produced by **1** on both duplex and quadruplex was found to be concentration dependent (Figure S4a,b). Interestingly, only in the case of *h-Telo* a significant stabilisation was observed at increasing concentration of **1**, reaching $\Delta T_{1/2}$ values even higher than the one obtained with the control molecule TMPyP4, a porphyrin known to be a good G4 binder, though with poor selectivity.[22]

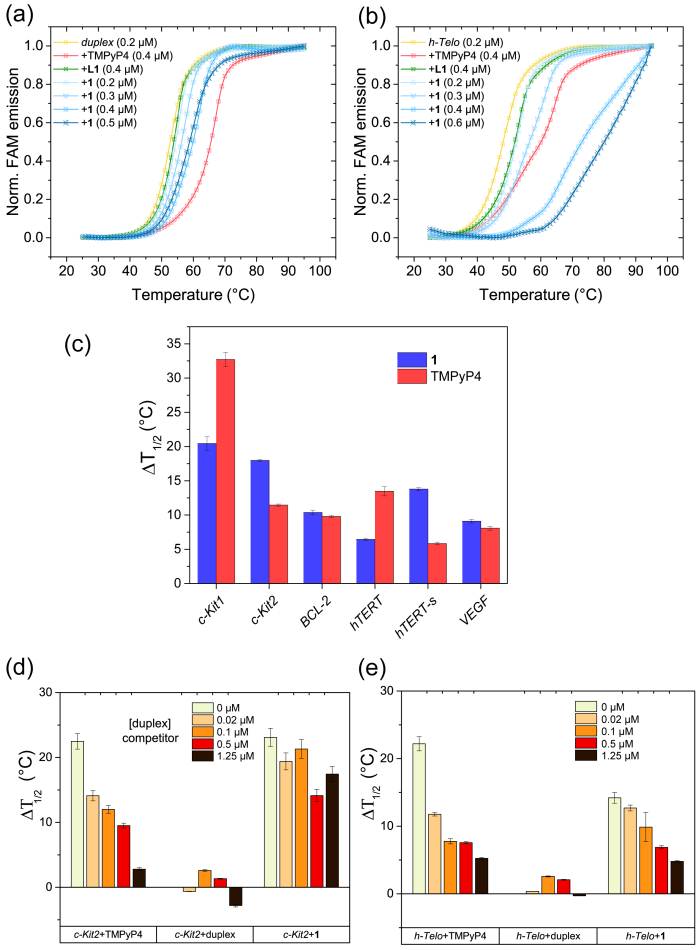

Figure S4. Interaction with duplex DNA and G4 sequences. (a-b) FRET melting profiles of (a) *ds-DNA* duplex and (b) *h-Telo* G4 upon interaction with ligand **L1**, metallacycle **1** and control TMPyP4 at the indicated concentrations. Buffer: 60 mM potassium cacodylate, pH 7.4. (c) Bar graph representing stabilization temperatures, $\Delta T_{1/2}$ (°C), obtained by FRET melting assays for **1** and TMPyP4 (0.4 μM) binding to the investigated G4 sequences (0.2 μM). Buffer: 60 mM potassium cacodylate, pH 7.4. (d-e) Stabilization of (d) *c-Kit2* and (e) *h-Telo* G4s (0.2 μM) by **1** (0.5 μM) and control compound TMPyP4 (0.5 μM) in the presence of increasing concentration of duplex DNA competitor (ct-DNA). Concentration of G4s are reported per strand; ct-DNA concentration has been divided by 20 (average base length of a G4 sequence) to make a fair comparison for selectivity. For the competition assay, 10 mM potassium cacodylate buffer (pH 7.4) supplemented with 95 mM of LiCl was used.[22]

Encouraged by these results, other FRET melting assays were performed using **1** (and control TMPyP4) with G-rich oncogene sequences known to fold in G4s with different arrangements (Figure S4c). Interestingly, compound **1** turned out to be more active than the porphyrin when bound to *c-Kit2* and *hTERT-s* oligonucleotides, which form standard parallel G4s.[23,24] An opposite situation was observed when the metallacycle was mixed with *c-Kit1* and *hTERT* sequences, known to form a parallel quadruplex with a unique cleft,[25] and a parallel G4 with a 26-base long looping hairpin,[24] respectively. These findings would suggest that **1** interacts preferentially via stacking on the guanine quartets while the presence of loops and/or cavities on the G4 secondary structure likely diminishes its affinity.

Competitive FRET experiments were performed using the *c-Kit2*-**1** and *h-Telo*-**1** systems in the presence of increasing amounts of duplex-DNA. *c-Kit2* thermal stabilization induced by **1** was less affected by the duplex competitor when compared with TMPyP4 (Figure S4d). On the other hand, the addition of a duplex to the *h-Telo*-**1** system (Figure S4e) produced a clear destabilisation effect.

UV-Vis and fluorescence titrations were performed in order to quantify the interaction between **1** and duplex or G4 DNA models. The UV-Vis spectrum of compound **1** (solid black line, Figure S5a,b), when exposed to increasing concentrations of *c-Kit2,* showed a hypochromic effect accompanied by a large red-shift. These effects, especially the red shift, were less pronounced in the case of **1** interacting with the duplex model ct-DNA. At the same time, a strong fluorescence quenching was observed after the interaction of **1** with the same parallel G4 in solution (Figure S6a) and the duplex model *ds-DNA* (Figure S6b). Stern-Volmer constants (Figure S6c) revealed that the quenching effect was one order of magnitude lower the interaction with *ds-DNA*. Binding constants (K_b) have been calculated from UV-Vis and fluorescence titrations and in both cases the interaction with the quadruplex motif *c-Kit2* resulted higher of one to two order of magnitude.

Overall, these thermal and spectroscopic data suggest that, while it is true that metallacycle **1** binds both duplexes and quadruplexes, it can be said that the platinum compound has a moderate preference for (parallel) G4s, behaving better than the poorly selective TMPyP4.

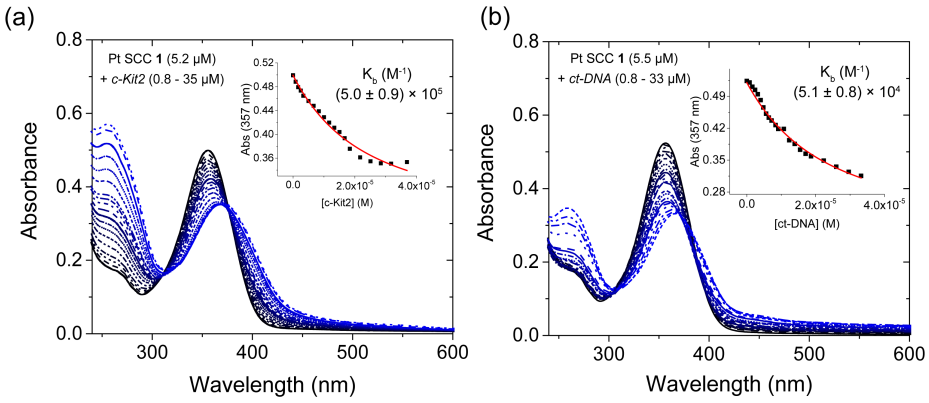

Figure S5. UV-Vis titrations. (a-b) UV-Vis absorption spectrum of **1** in combination with increasing amount of (a) *c-Kit2* G4 and (b) ct-DNA. In the insets the plot of the absorbance at 357 nm for the calculation of the binding constants (K_b). K_b values have been calculated using previously reported equations, and the related fitting was obtained implementing such equations in Origin software.[26] Buffer: Tris-HCl 5 mM, KCl 50 mM, pH=7.8.

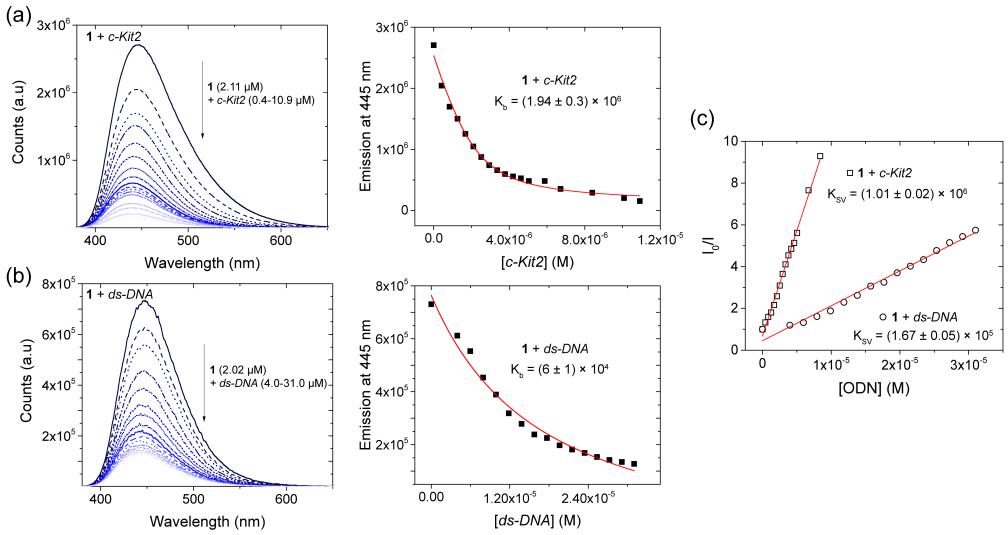

Figure S6. Emission of 1 interacting with G4 and B-DNA. Fluorescence titration of compound **1** with increasing amounts of (a) *c-Kit2* and (b) *ds-DNA* sequences in Tris-HCl 5 mM, KCl 50 mM, pH=7.8. λ_{exc} = 360 nm, Slits width = 5.0/0.6 nm for *c-Kit2* and 0.6/0.6 nm for *ds-DNA*. In the right column the plot of the emission at 445 nm for the calculation of the binding constants. (c) Stern-Volmer plots for fluorescence quenching of **1** by *c-Kit2* and *ds-DNA* oligonucleotides. Binding (K_b) and Stern-Volmer constants (K_{SV}) have been calculated using previously reported equations, and the related fitting was obtained implementing such equations in Origin software.[26,27] For Stern-Volmer data fitting, only the linear portion of the plot was used. Concentration of the ODNs are reported in bases.

Circular dichroism measurements and docking calculations were performed to give insights on the metallacycle mode of binding to DNA. The addition of increasing aliquots of **1** to a *c-Kit2* solution induced the appearance of a slight CD band at around 380 nm, without dramatic shifts in the quadruplex fingerprint region of the spectrum (200-300 nm), indicating that the general parallel arrangement of the G4 is preserved after the interaction (probably via stacking on top of the tetrads) (Figure S7a). This scenario is confirmed by docking simulations (Figure S7c) where metallacycle **1** uses one of its viologen chromophores to sit on top of the terminal G-tetrad. It is worth noting that both CD and simulations indicated that **1** acts as a major groove binder when interacting with duplex DNA (Figures S7b and S7d).

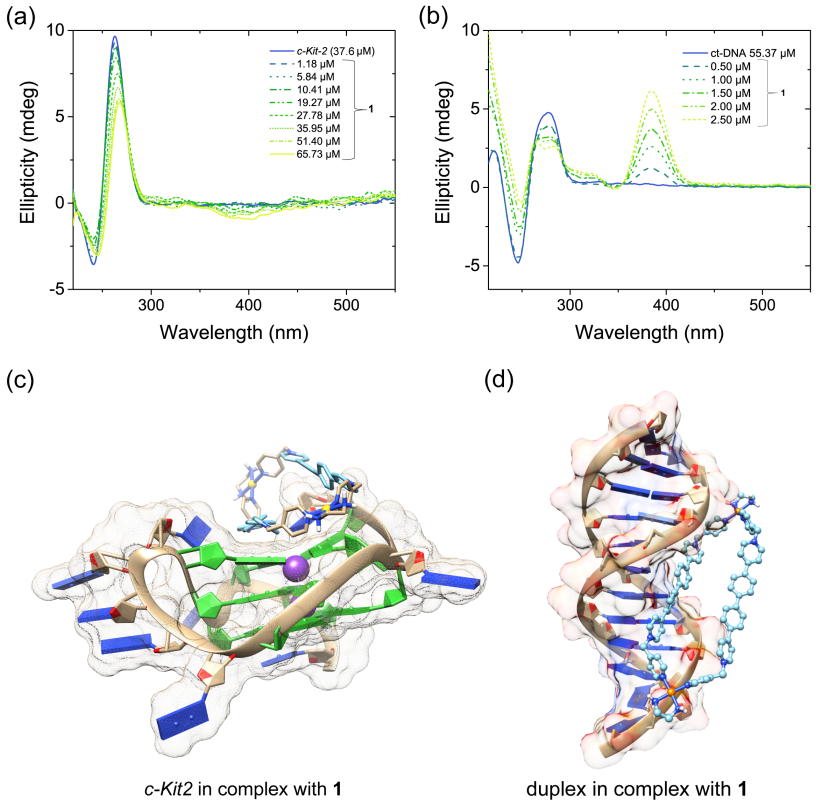

Figure S7. Circular dichroism and docking calculations. (a-b) CD spectra of (a) *c-Kit2* G4 and (b) ct-DNA in the presence of increasing aliquots of metallacycle **1**. Concentrations of both *c-Kit2* and ct-DNA are reported in bases. Buffer: Tris-HCl 5 mM, KCl 50 mM, pH=7.8. (c-d) Cartoon showing the best docking binding pose of **1** with (c) parallel G4 *c-Kit2* (PDB entry 2KQH) and (d) a duplex DNA model (PDB entry 1BNA).

Cell studies

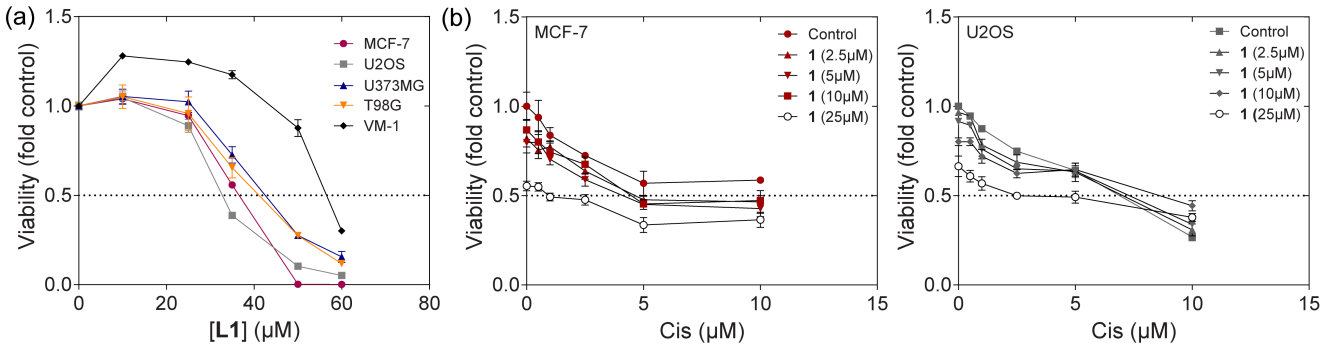

Figure S8. Impact of L1 and 1 in combination with cisplatin on cancer cell viability. (a) Viability of U2OS, MCF-7, U373MG, T98G and VM-1 cells was assessed by MTT assay following 72h exposure to increasing **L1** concentrations in the range of 0-50 μM. Data are normalized to untreated controls. The dashed line refers to 50% cell viability and indicates the IC_{50}. Each data point represents the mean ± SD of three replicates of one representative experiment, which was performed at least three times. (b) Impact of **1** at the indicated concentrations on the activity of cisplatin (Cis) was assessed under conditions as in (a). Cell viability was in these experiments assessed by CellTiter-Glo® Luminescent Cell Viability Assay (Promega) detecting cellular ATP contents following the instructions of the manufacturer.

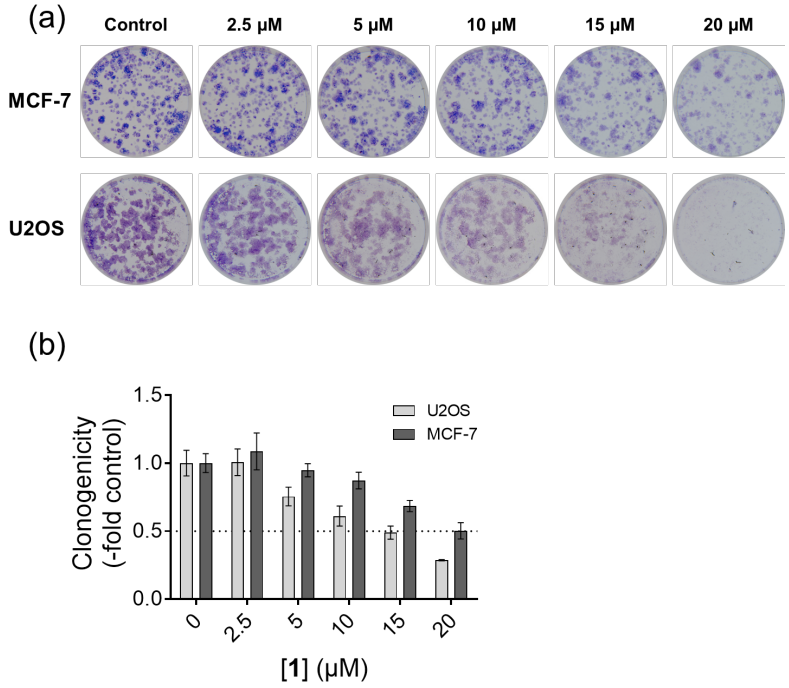

Figure S9. Impact of metallacycle 1 on the colony formation capacity of MCF-7 and U2OS cells. $1x10^3$ (U2OS) or $2x10^3$ (MCF-7) cells/ml were exposed for 7 days to increasing concentrations of **1** (0-20 µM). (a) Representative pictures after MeOH fixation and crystal violet staining upon treatment with the indicated drug concentrations taken with a Nikon Digital Camera D3200. The upper panel refers to MCF-7 cells, the lower panel to U2OS cells. (b) Colony growth of U2OS and MCF-7 cells given as relative integrated density values normalized to the untreated controls, quantified with ImageJ 1.51f software and illustrated as bar graphs with GraphPad Prism 5.0 software. The dashed line refers to 50% colony forming capacity. Bars indicate duplicate values of one representative experiment, performed at least three times and are presented as mean ± SD.

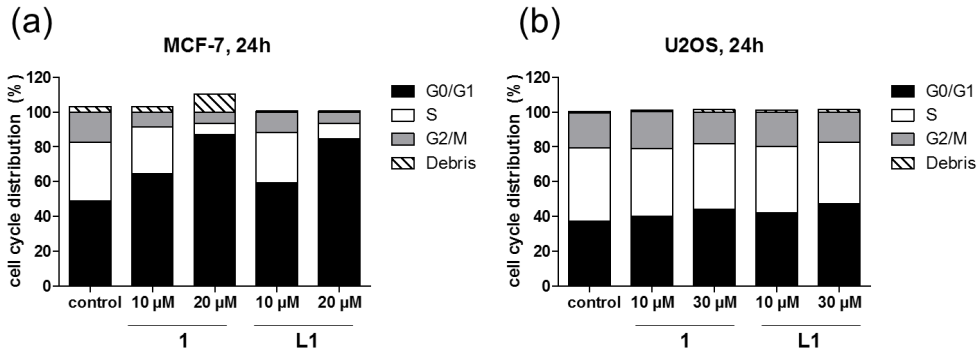

Figure S10. Effects on cell cycle distribution upon treatment with 1 and L1. (a) MCF-7 and (b) U2OS cells were exposed for 24 h with either (a) 10 and 20 µM or (b) 10 and 30 µM of the indicated compounds. DNA content of the cells was measured following EtOH fixation and PI staining with flow cytometry and quantified with the Cell Quest Pro Software. Data are presented as number of cells (%) in G0/G1, S and G2/M phase using GraphPad Prism 5.0 software and refer to one representative experiment, which was performed at least three times.

(a)

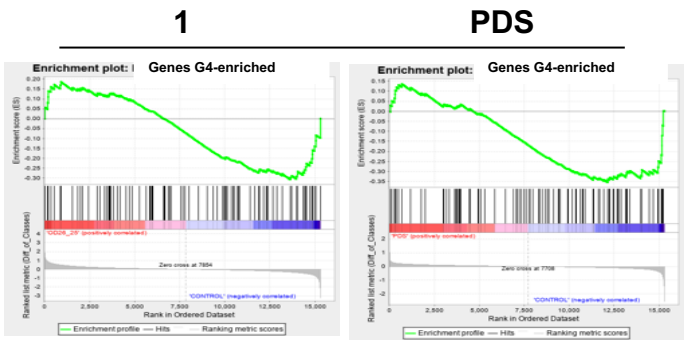
1
PDS
Enrichment plot: Genes G4-enriched
Enrichment plot: Genes G4-enriched

(b)

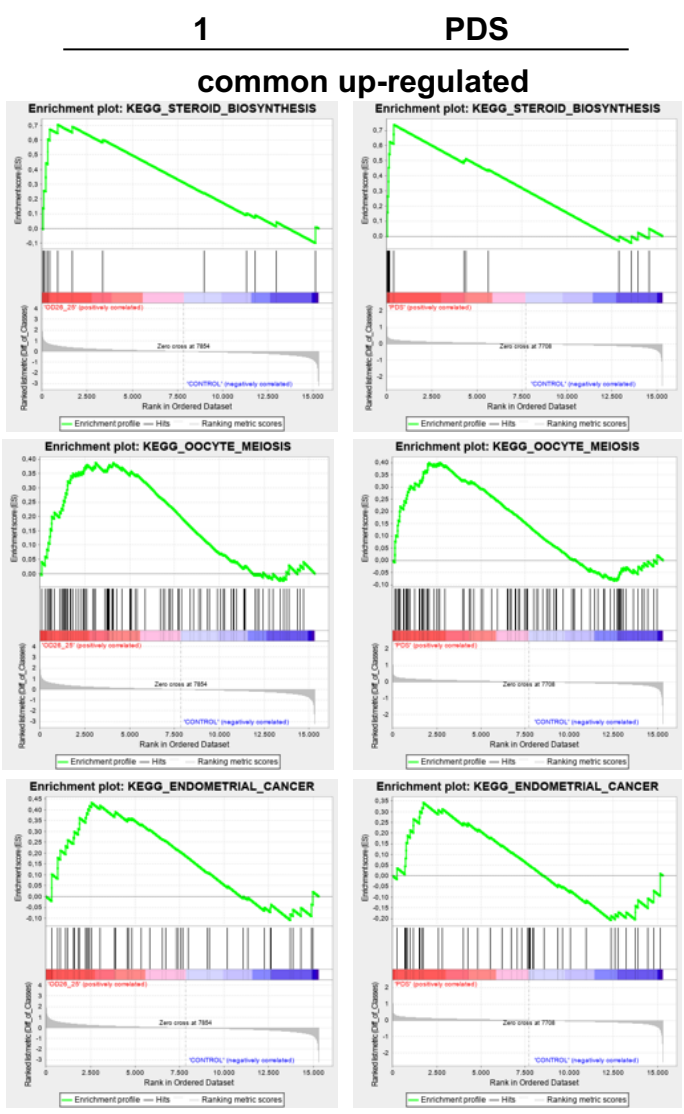
1
PDS
common up-regulated
Enrichment plot: KEGG_STEROID_BIOSYNTHESIS
Enrichment plot: KEGG_STEROID_BIOSYNTHESIS
Enrichment plot: KEGG_OOCYTE_MEIOSIS
Enrichment plot: KEGG_OOCYTE_MEIOSIS
Enrichment plot: KEGG_ENDOMETRIAL_CANCER
Enrichment plot: KEGG_ENDOMETRIAL_CANCER

(c)

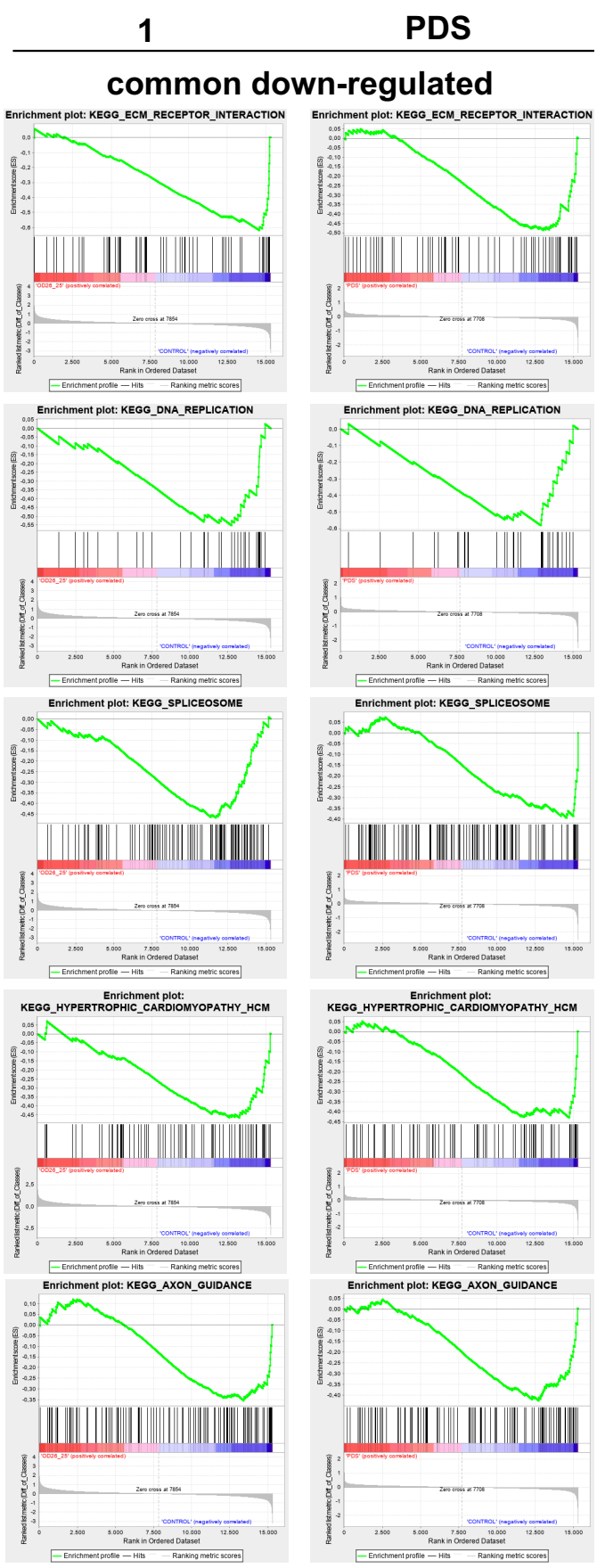

Figure S11. (a) Impact of **1** and PDS (24 h exposure, 25 μM and 15 μM, respectively) on the expression of genes in chromosomal regions enriched for G4 structures as published by Lam et al. (Nat. Commun. 2013, 4, 1796). (b,c) Selection of representative KEGG pathways significantly upregulated (b) or downregulated (c) by **1** and PDS (24 h exposure, 25 μM and 15 μM, respectively). GSEA analyses were performed using http://www.broadinstitute.org/gsea/msigdb/index.jsp

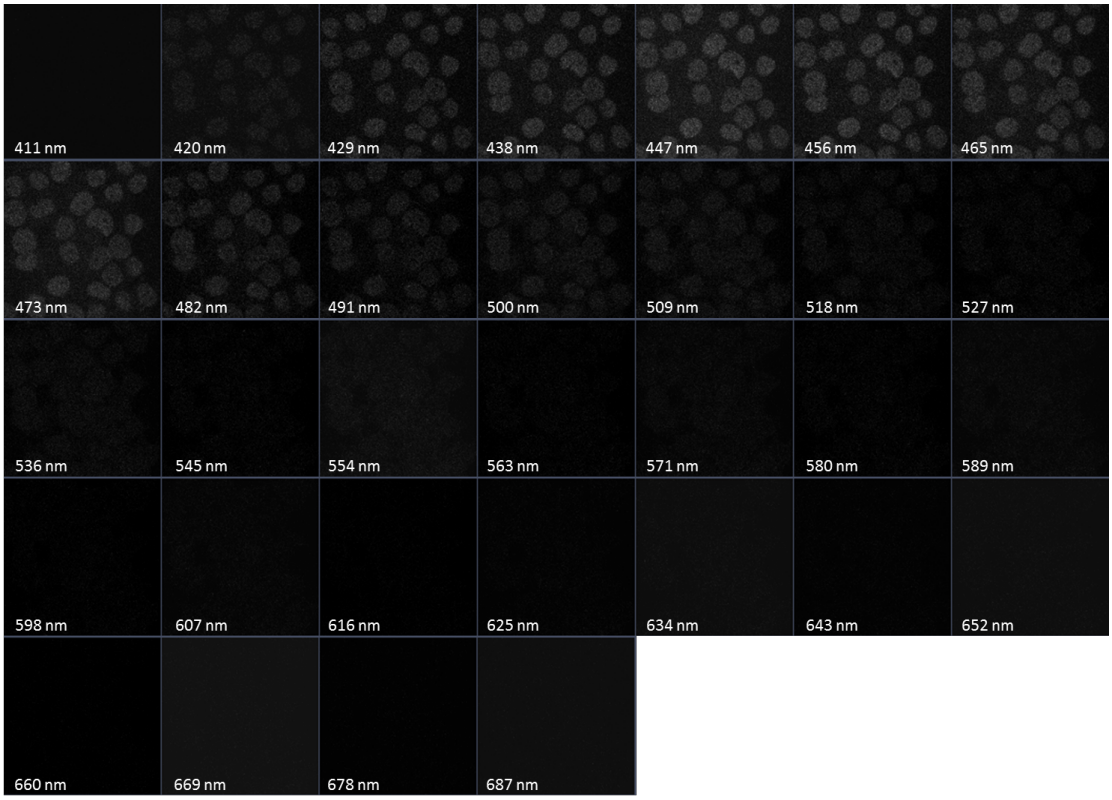

Figure S12. Fluorescence emission fingerprinting of 1. MCF-7 cells treated with 50 µM **1** were employed for the acquisition of a series of *x-y* images with a Zeiss LSM 780 confocal laser scanning microscope and Zen 2.3 SP1 software using a Plan-Apochromat 63×/1.4 NA Oil DIC M27 objective. The emission of **1** was acquired after excitation with 405 nm laser in the range of 411–687 nm and a bandwidth of 9 nm.

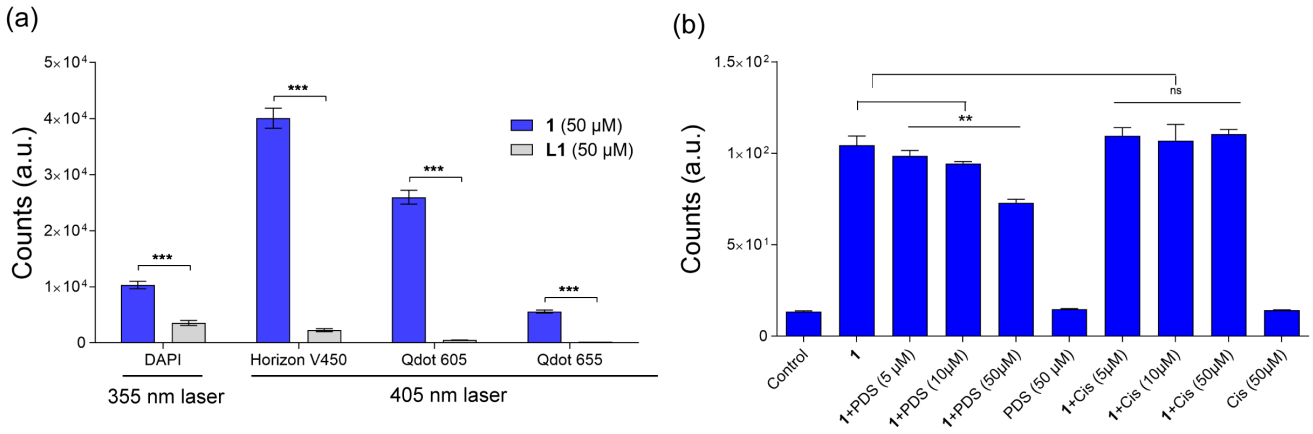

Figure S13. Intracellular fluorescence properties of 1 and L1. (a) Fluorescence intensity after 1h exposure of 50 µM **1** (blue) and **L1** (grey) in viable U2OS cells determined by flow cytometry and normalized to negative control. Emission signals were detected after excitation with the 355 nm laser in the DAPI channel (450/50 nm filter) and after excitation with the 405 nm laser in the Horizon V450 (450/50 nm filter), Qdot 605 (605/12 nm filter) as well as in the Qdot 655 (655/8 nm filter) channel. *** $p \leq 0.001$, DF=4, Student's t-test. (b) Live MCF-7 cells were exposed to 5 µM **1** in combination with the indicated concentrations of either the G-quadruplex stabilizer Pyridostatin (PDS) or the DNA targeting platinum anticancer drug cisplatin (Cis). Cellular fluorescence activity was determined by flow cytometry as under (a). **, $p < 0.01$ by One-way ANOVA with posthoc Bonferroni correction.

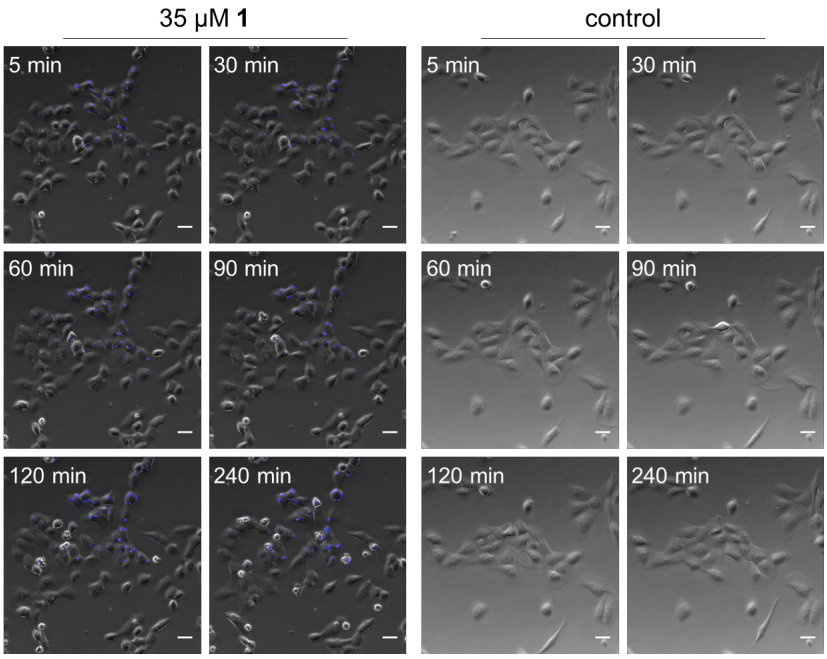

Figure S14. Time-dependent intracellular accumulation of 1. Representative merged images of live cell microscopy showing metallacycle **1** in U2OS cells (λ_{exc} = 395/25nm, λ_{em} = 460/50 nm). Scale bars indicate 25 µm.

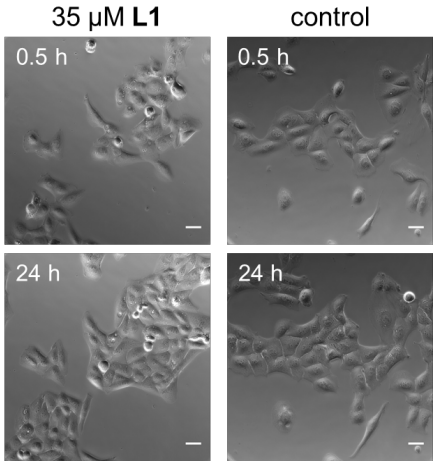

Figure S15. Time-dependent intracellular accumulation of L1. Representative merged images of live cell microscopy of ligand **L1** in U2OS cells (λ_{exc} = 395/25 nm, λ_{em} = 460/50 nm). Scale bars indicate 25 µm.

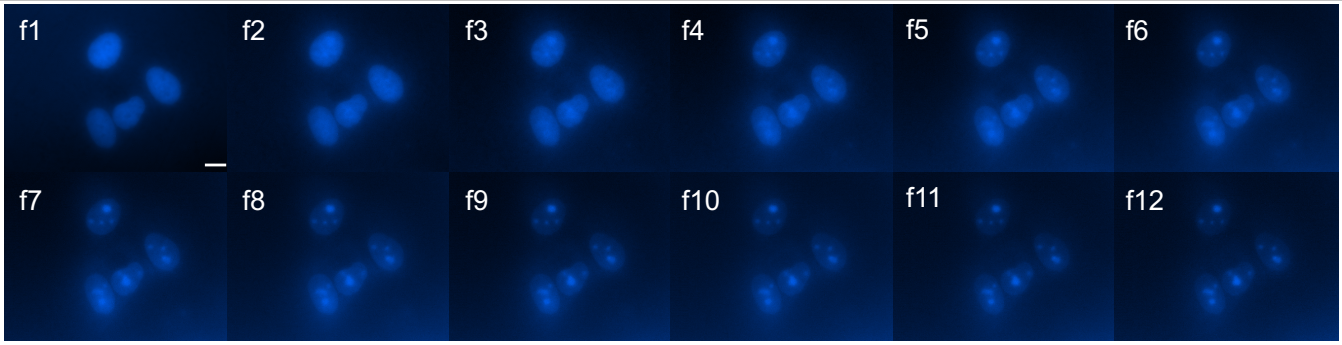

Figure S16. Selective photobleaching of 1-associated nuclear fluorescence. MeOH-fixed U2OS cells were stained with 5 µM **1** for 30 minutes. Fluorescence images were taken on a DMRXA (Leica, Wetzlar, Germany) with a PL APO 100x (1.4 – 0.7) oil objective in time-lapse mode with one frame every 5 seconds at an illumination time of 10 ms and the DAPI filter cube (350/50 excitation, 460/50 emission). Photomicrographs were processed by VisiView software (Visitron Systems, Puchheim, Germany) at Max/Min (range) autoscale settings each. Scale bar indicates 10 µm.

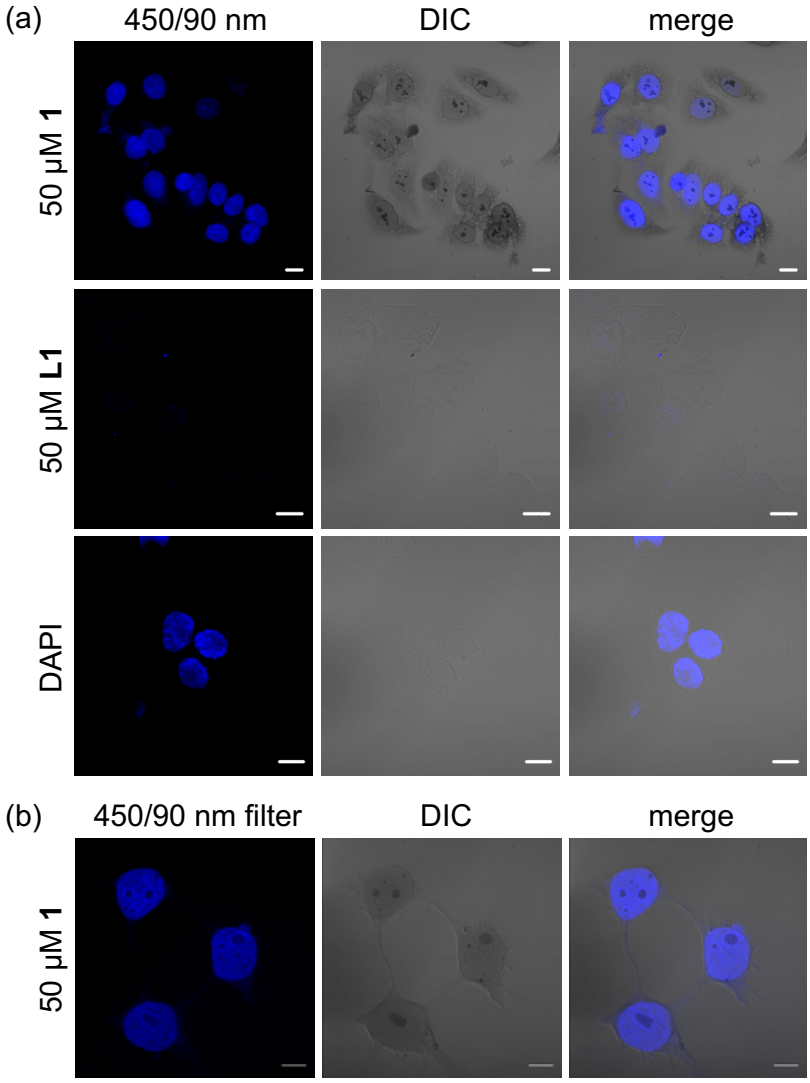

Figure S17. Visualization of 1, L1 and DAPI within PFA fixed cells and of 1 within MeOH fixed cells. (a) Representative images of U2OS cells incubated with 50 µM **1**, 50 µM **L1** or 1 µg/ml DAPI and (b) of MCF-7 cells stained with 50 µM **1** for 30 min. All cells were analyzed with CLSM using the 405 nm laser line and a Plan-Apochromat 63×/1.4 NA Oil DIC M27 objective. Scale bars indicate 10 µm.

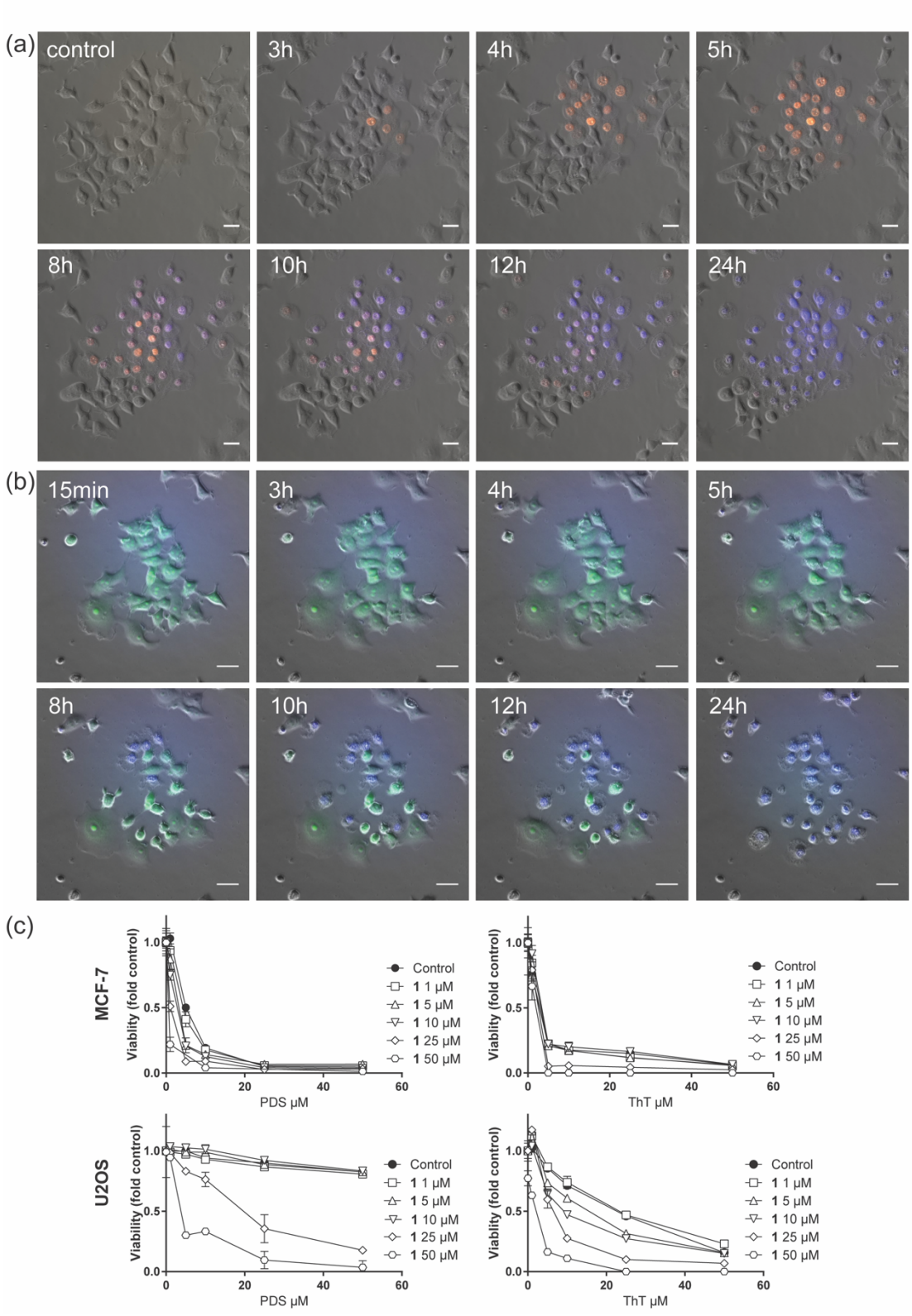

Figure S18. Competition of 1 and TMPyP4 or ThT for the same nuclear target. (a) Representative images of live cell microscopy showing time-dependent intracellular accumulation of TMPyP4 and metallacycle **1** within MCF-7 cells (λ_{exc} = 395/25nm, λ_{em} = 460/50 nm for the blue and λ_{exc} = 560/40nm, λ_{em} = 630/75nm for the red channel). Scale bars indicate 25 µm. See complete live cell competition in Video S1 (58 pictures, one every 30 min). (b) Representative images of live cell microscopy showing intracellular competition of ThT and **1** within U2OS cells. (λ_{exc} = 395/25nm, λ_{em} = 460/50 nm for the blue and λ_{exc} = 475/34, λ_{em} = 525/50 nm for the green channel). Scale bars indicate 10 µm. See complete live cell competition in Video S2 (95 pictures, one every 15 min). (c) **1** exerts synergistic activity with G4-targeting agents ThT and PDS in a 72h co-exposure experiment. Cell viability was determined by MTT assay. To focus on drug interaction effects, data in all curves are depicted normalized to the respective control containing medium (control) or the respective concentrations of **1** as indicated.

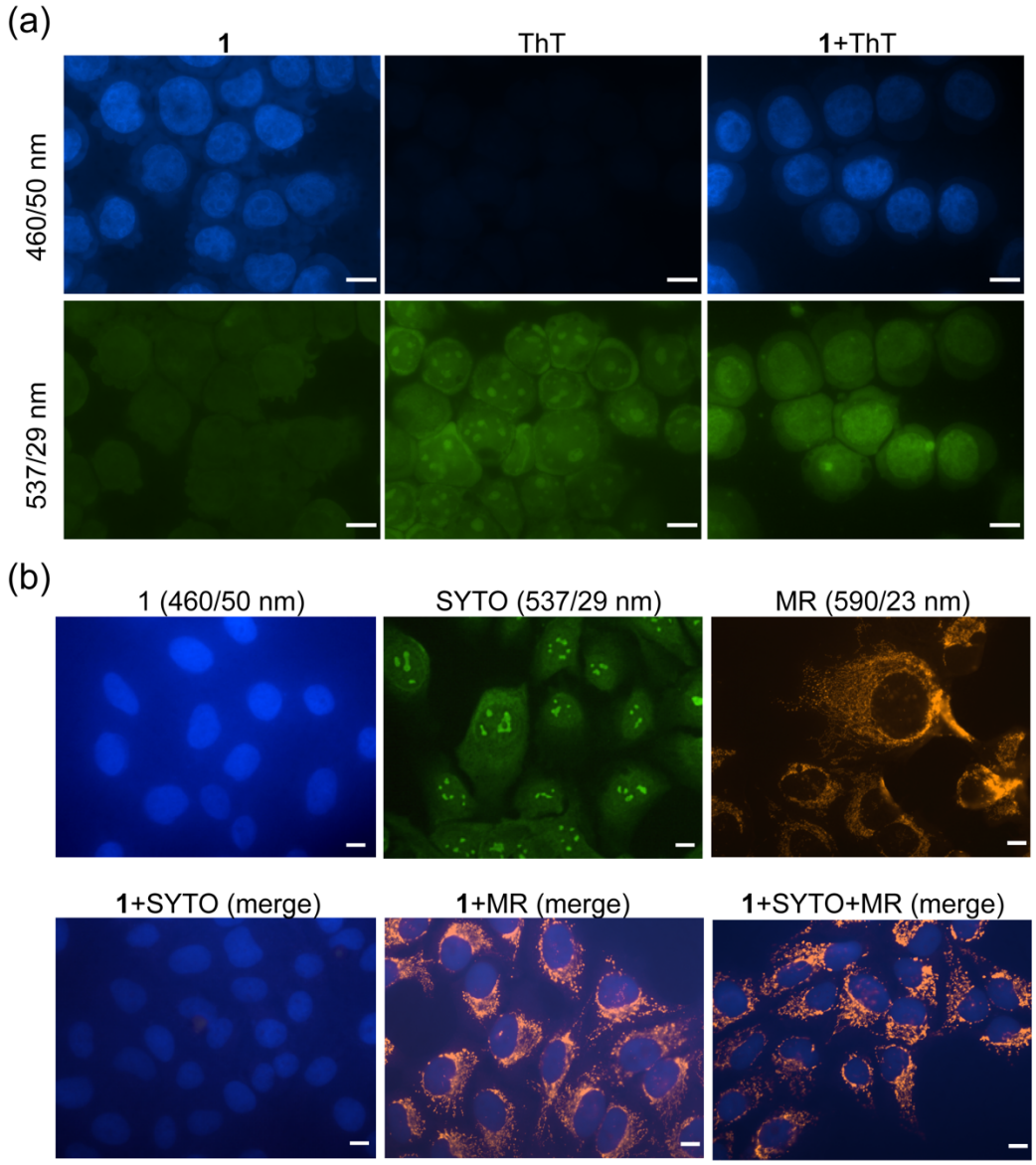

Figure S19. Co-labelling with 1 and ThT, SYTO and MR. (a) MCF7 cells were cytospin prepared, fixed in MeOH (-20°C, 15min) and consequently stained with **1** (5 µM), ThT (5 µM) or a combination of both as indicated. (b) U2OS cells were grown on Ibidi 8-well µ-slides for 24h and then exposed to either SYTO® RNASelect green fluorescence nucleoli dye (SYTO 500 nM; Molecular Probes, Eugene, OR) or MitoTracker® Red CMXRos (MR, 250 nM; Molecular Probes) for 30 min. Then cells were fixed in MeOH (-20°C, 15 min) and stained with **1** (5 µM). Fluorescence images were taken on a DMRXA (Leica, Wetzlar, Germany) with a HCX PL APO 63x (1.32 – 0.6) oil objective using DAPI (λ_{exc} 350/50, λ_{em} 460/50), FITC (λ_{exc} 495/25, λ_{em} 537/29), or Cy3 (λ_{exc} 546/22, λ_{em} 590/23) filter cubes. In (b) acquisition setting were kept identical for the single dye photomicrographs in the upper and the merged pictures in the lower panels. Photomicrographs were processed by VisiView software (Visitron Systems, Puchheim, Germany) in all cases at 14 bit full range settings. Scale bars indicate 10 µm.

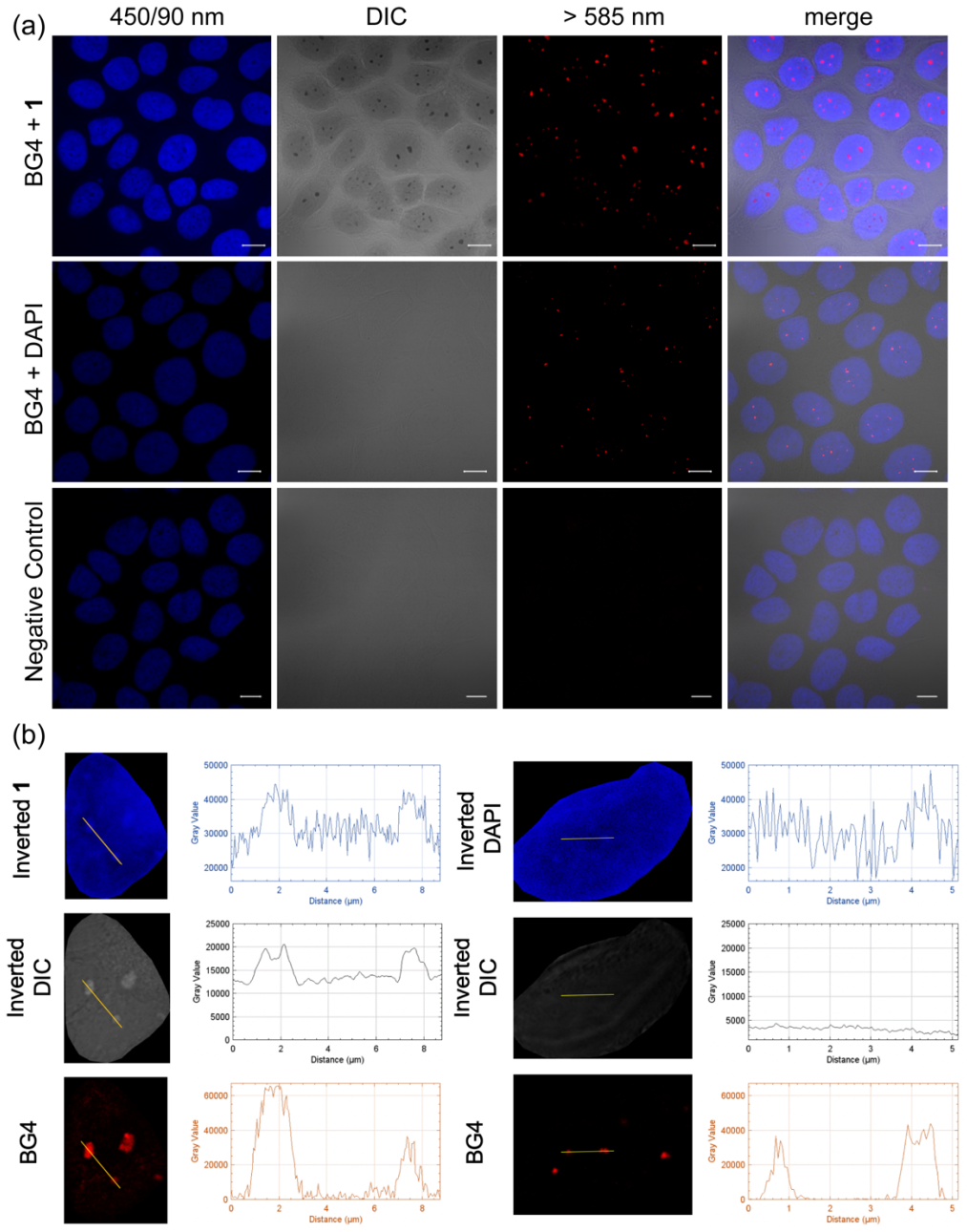

Figure S20. (a) **Colocalization of 1 and BG4**. Representative CLSM images of immunofluorescence staining with BG4 (red) on MeOH fixed MCF-7 cells, counterstained with **1** or DAPI (blue). Scale bars indicate 10 µm. (b) Analysis of spatial correlation of nuclear fluorescence, DIC absorption, and G4-enriched chromatin regions of **1**-treated versus DAPI-stained MCF-7 cells shown in Figure 3a. Two-dimensional pixel intensity plots from the indicated yellow lines in fluorescence and DIC channels of representative cropped nuclei of 1-treated cells (left panel) and DAPI-stained cells (right panel) were generated using the "Plot Profile" analysis tool in ImageJ software. X-axes of intensity plots indicate the distance along respective yellow lines. Y-axes indicate pixel intensities of each channel (16-bit image depth) along respective yellow lines.

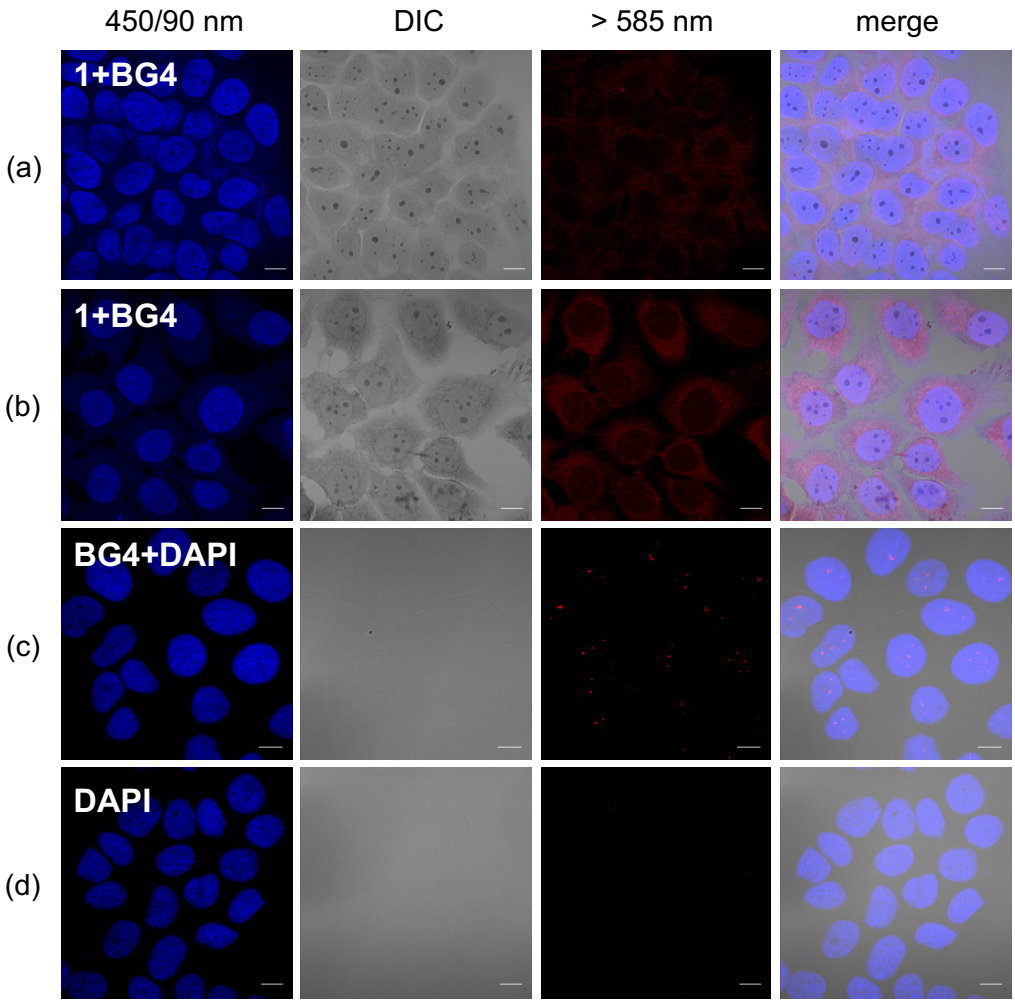

Figure S21. **Treatment with 1 disrupts epitope recognition by BG4 in MeOH-fixed cells.** (a) MeOH-fixed MCF-7 cells, treated with 50 μM **1** for 30 min followed by BG4 incubation. (b) 50 μM **1** pre-treated MCF-7 cells (1 h), fixed with MeOH and stained with BG4. (c) Confocal microscopy pictures of untreated MCF-7 cells, fixed with MeOH and stained with BG4 (positive control). (d) AF594 negative control. Control pictures are counterstained with DAPI (blue). Scale bars indicate 10 μm.

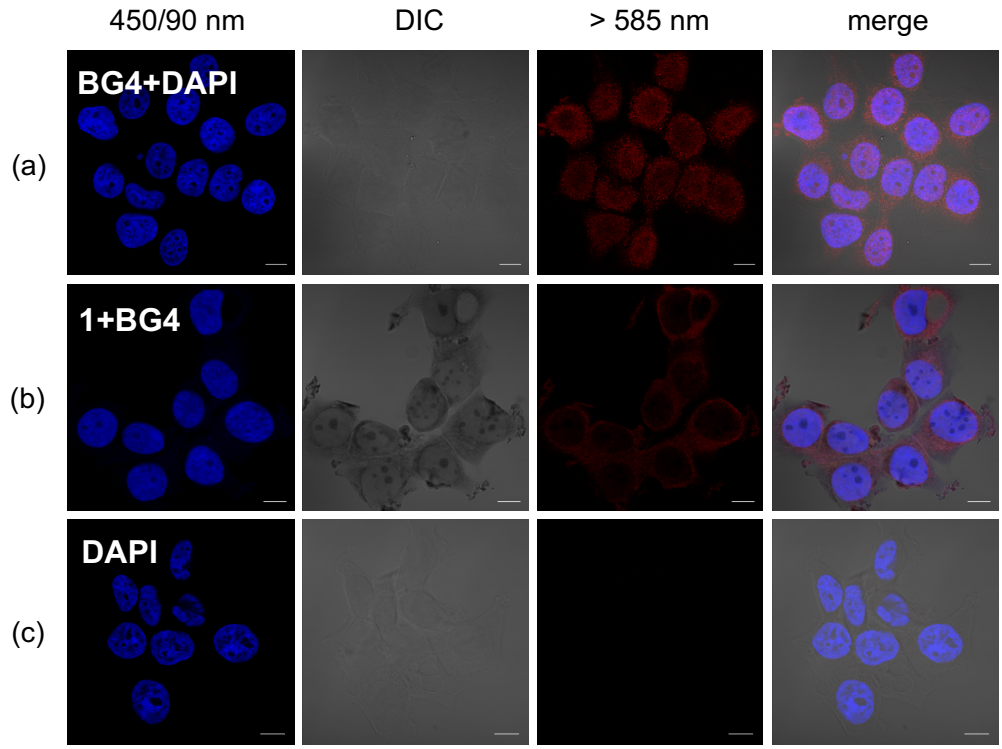

Figure S22. **Treatment with 1 disrupts epitope recognition by BG4 in PFA-fixed cells.** (a) MCF-7 cells fixed with PFA, incubated with BG4 and counterstained with DAPI showed a nuclear red punctate staining pattern (partially extended to the cytoplasm as previously reported.[15,16] (b) When PFA-fixed MCF-7 cells were treated with metallacycle **1** (50 μM) for 30 min before BG4 incubation, the punctate pattern got diffused, appearing enriched in the cytoplasm. (c) AF594 negative control, counterstained with DAPI. Scale bars indicate 10 μm.

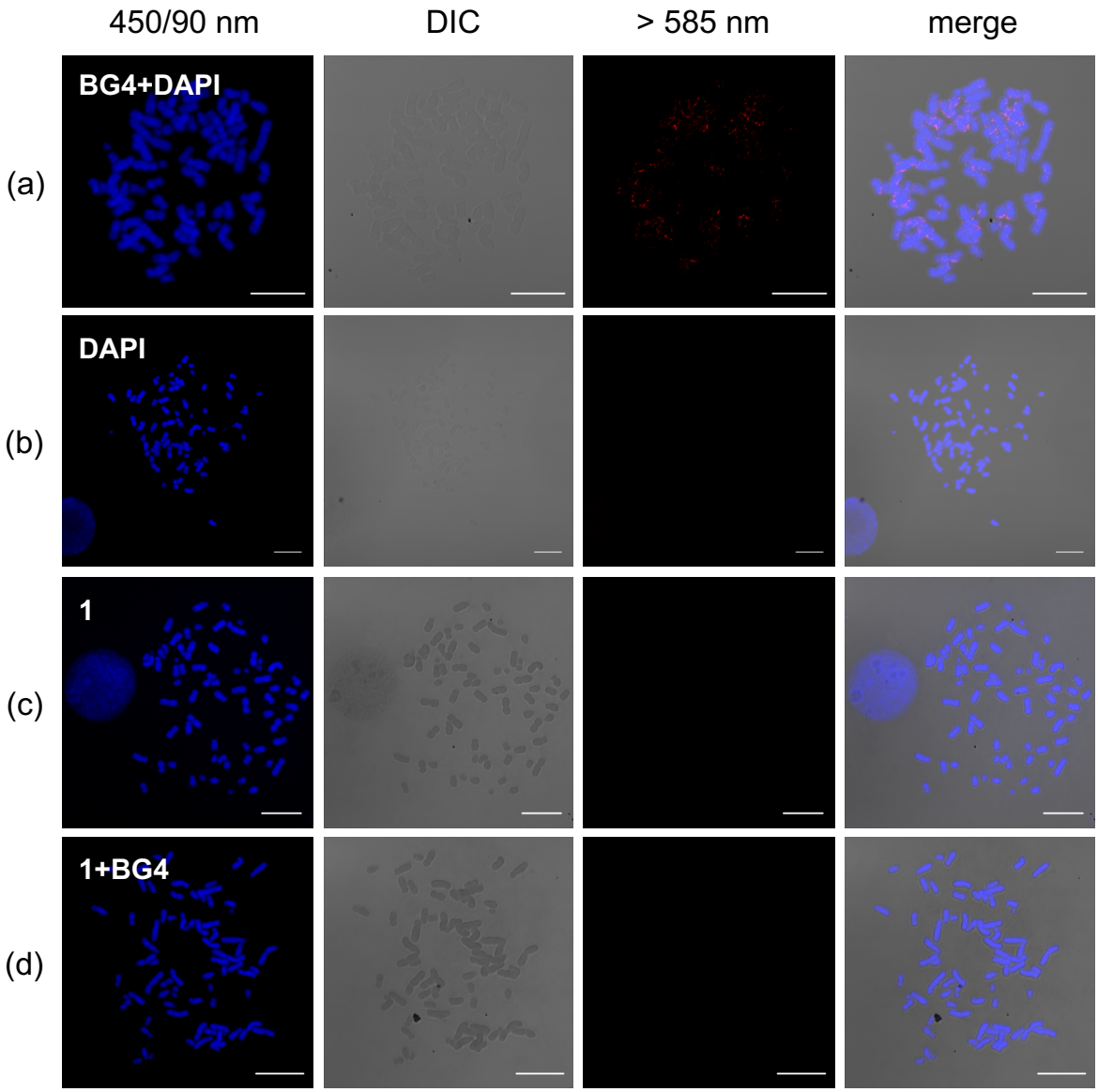

Figure S23. **Detection of G-quadruplex structures in metaphase chromosomes of human cancer cells.** (a) Representative confocal images of immunofluorescence staining with BG4 (red) and DAPI (blue) on MCF-7 metaphase chromosome spreads. Metaphase chromosomes i immune-stained with BG4 showed distinct red foci at both telomeres and non-telomeric regions, as previously reported).[15] (b) AF594 negative control, counterstained with DAPI. (c) Confocal images of MCF-7 chromosomes stained with 50 μM **1** for 30 minutes**.** (d) MCF-7 chromosomes treated with 50 μM **1** for 30 min followed by BG4 incubation. Images were acquired using 405 nm excitation laser line and a Plan-Apochromat 63×/1.4 NA Oil DIC M27 objective. Scale bars indicate 10 μm.

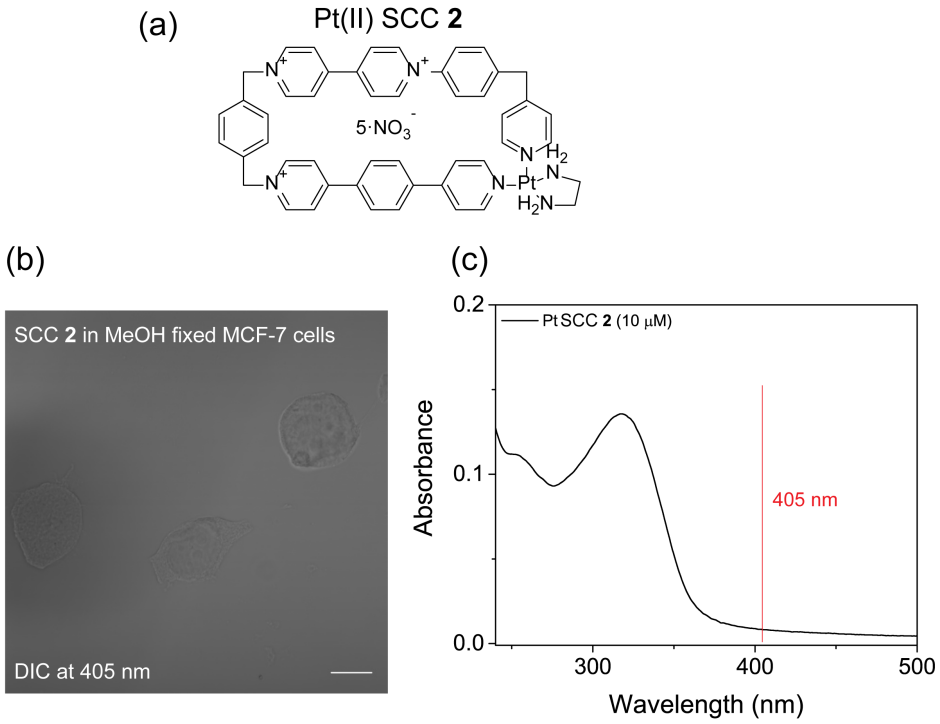

Figure S24. Absorption features of 2 in cell and in solution. (a) Structure of Pt(II) SCC **2**. (b) Bright field image of MeOH fixed MCF-7 cells incubated with Pt-metallacycle **2** acquired using transmitted light DIC mode with the 405 nm laser line and a Plan-Apochromat 63×/1.4 NA Oil DIC M27 objective. (c) UV-Vis absorption spectrum of **2** in Tris-HCl 5 mM, KCl 50 mM, pH=7.8.

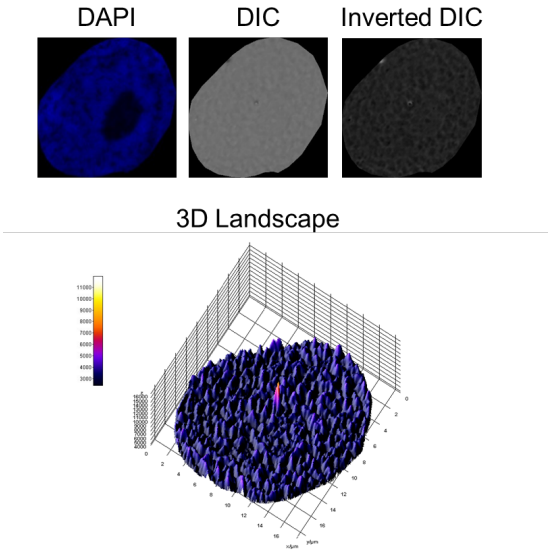

Figure S25. DAPI control experiment in DIC mode. Representative nucleus cropped from confocal image of MCF-7 cells fixed with MeOH and incubated with DAPI and acquired using transmitted light DIC mode at 405 nm. Differences in absorption within subnuclear regions were visualized by three-dimensional surface plotting of single pixel intensities of the inverted DIC image.

References

[1] O. Domarco, I. Neira, T. Rama, A. Blanco-Gómez, M. D. García, C. Peinador, J. M. Quintela, *Org. Biomol. Chem.* **2017**, *15*, 3594–3602.

[2] C. A. Schneider, W. S. Rasband, K. W. Eliceiri, *Nat. Methods* **2012**, *9*, 671–675.

[3] D. Renčiuk, J.-L. Mergny, A. Guédin, J. Zhou, L. Beaurepaire, A. Bourdoncle, *Methods* **2012**, *57*, 122–128.

[4] O. Trott, A. J. Olson, *J. Comput. Chem.* **2010**, *31*, 455–61.

[5] A. D. Becke, *J. Chem. Phys.* **1993**, *98*, 5648–5652.

[6] C. Lee, W. Yang, R. G. Parr, *Phys. Rev. B* **1988**, *37*, 785–789.

[7] P. J. Stephens, F. J. Devlin, C. F. Chabalowski, M. J. Frisch, *J. Phys. Chem.* **1994**, *98*, 11623–11627.

[8] P. J. Hay, W. R. Wadt, *J. Chem. Phys.* **1985**, *82*, 270–283.

[9] P. C. Hariharan, J. A. Pople, *Theor. Chim. Acta* **1973**, *28*, 213–222.

[10] M. M. Francl, *J. Chem. Phys.* **1982**, *77*, 3654–3665.

[11] M. J. Frisch, G. W. Trucks, H. B. Schlegel, G. E. Scuseria, M. A. Robb, J. R. Cheeseman, G. Scalmani, V. Barone, B. Mennucci, G. A. Petersson, et al., *Gaussian Inc Wallingford CT* **2009**, *34*, Wallingford CT.

[12] G. M. Morris, R. Huey, W. Lindstrom, M. F. Sanner, R. K. Belew, D. S. Goodsell, A. J. Olson, *J. Comput. Chem.* **2009**, *30*, 2785–2791.

[13] E. F. Pettersen, T. D. Goddard, C. C. Huang, G. S. Couch, D. M. Greenblatt, E. C. Meng, T. E. Ferrin, *J. Comput. Chem.* **2004**, *25*, 1605–1612.

[14] C. Pirker, K. Holzmann, S. Spiegl-Kreinecker, L. Elbling, C. Thallinger, H. Pehamberger, M. Micksche, W. Berger, *Melanoma Res.* **2003**, *13*, 483–492.

[15] G. Biffi, D. Tannahill, J. McCafferty, S. Balasubramanian, *Nat. Chem.* **2013**, *5*, 182–186.

[16] G. Biffi, M. Di Antonio, D. Tannahill, S. Balasubramanian, *Nat. Chem.* **2014**, *6*, 75–80.

[17] V. Mathieu, C. Pirker, W. M. Schmidt, S. Spiegl-Kreinecker, D. Lötsch, P. Heffeter, B. Hegedus, M. Grusch, R. Kiss, W. Berger, *Oncotarget* **2012**, *3*, 399–413.

[18] E. Puujalka, M. Heinz, B. Hoesel, P. Friedl, B. Schweighofer, J. Wenzina, C. Pirker, J. A. Schmid, R. Loewe, E. F. Wagner, et al., *J. Invest. Dermatol.* **2016**, *136*, 967–977.

[19] E. Y. N. Lam, D. Beraldi, D. Tannahill, S. Balasubramanian, *Nat. Commun.* **2013**, *4*, 1796.

[20] V. Mathieu, C. Pirker, W. M. Schmidt, S. Spiegl-Kreinecker, D. Lötsch, P. Heffeter, B. Hegedus, M. Grusch, R. Kiss, W. Berger, *Oncotarget* **2012**, *3*, 399–413.

[21] J. Dai, C. Punchihewa, A. Ambrus, D. Chen, R. A. Jones, D. Yang, *Nucleic Acids Res.* **2007**, *35*, 2440–2450.

[22] J. M. Nicoludis, S. P. Barrett, J. L. Mergny, L. A. Yatsunyk, *Nucleic Acids Res.* **2012**, *40*, 5432–5447.

[23] S. T. D. Hsu, P. Varnai, A. Bugaut, A. P. Reszka, S. Neidle, S. Balasubramanian, *J. Am. Chem. Soc.* **2009**, *131*, 13399–13409.

[24] S. M. L. Palumbo, S. W. Ebbinghaus, L. H. Hurley, *J. Am. Chem. Soc.* **2009**, *131*, 10878–10891.

[25] A. T. Phan, V. Kuryavyi, S. Burge, S. Neidle, D. J. Patel, *J. Am. Chem. Soc.* **2007**, *129*, 4386–4392.

[26] P. Thordarson, *Chem. Soc. Rev.* **2011**, *40*, 1305–1323.

[27] E. Rajczak, V. L. Pecoraro, B. Juskowiak, *Metallomics* **2017**, *9*, 1735–1744.

Author Contributions

A.T., W.B. and C.P. conceived and directed the study in all its parts. O.D. and M.D.G. performed the synthesis and the structural characterization of the metallacycle. O.D. and A.T. carried out all the measurements in solution. C.K, C.P. and C.D. performed the in-cell studies including cell viability and clonogenic assays, flow cytometry, live cell microscopy and CLSM. B.E., J.R. and G.T. analysed live cell microscopy and CLSM data. A.T., W.B., C.P. and B.K.K. analysed and interpreted the overall results. All the authors contributed to the final version of the manuscript.